THE ROLE OF BTB/ZINC FINGER TRANSCRIPTION FACTOR

PATZ1/MAZR IN THE REGULATION OF P53-MEDIATED DNA

DAMAGE RESPONSE DURING T CELL DEVELOPMENT

by

MANOLYA ÜN

Submitted to the Graduate School of Engineering and Natural Sciences
in partial fulfillment of
the requirements for the degree of
Master of Science

Sabancı University

Spring 2011

Sabancı Üniversitesi
Fen Bilimleri Enstitüsü
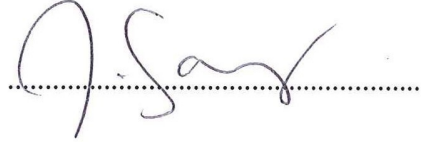
Yüksek Lisans Tez Sınavı Tutanağı

09.08.2011

Fen Bilimleri Enstitüsü yüksek lisans öğrencilerinden 13492 numaralı Manolya Ün'ün sözlü tez jüri sınavı 09.08.2011 tarihinde yapılmış ve adı geçen öğrencinin "The Role of BTB/Zinc Finger Transcription Factor PATZ1/MAZR in the Regulation of p53-mediated DNA Damage Response during T-Cell Development" başlıklı yüksek lisans tezi başarılı bulunarak juri tarafından kabul edilmiştir.

Tez Jüri üyeleri

1- Assoc. Prof. Batu Erman ....
   (Thesis Supervisor)

2- Prof. Dr. Zehra Sayers ....
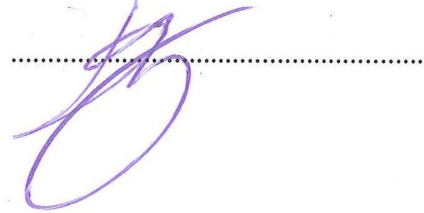
3- Prof. Dr. Ali Rana Atılgan ....

4- Assoc. Prof. Uğur O. Sezerman ....

5- Asst. Prof. Devrim Gözüaçık ....

THE ROLE OF BTB/ZINC FINGER TRANSCRIPTION FACTOR

PATZ1/MAZR IN THE REGULATION OF P53-MEDIATED DNA

DAMAGE RESPONSE DURING T CELL DEVELOPMENT

Manolya Ün

M.Sc. Thesis 2011

Thesis Supervisor: Assoc. Prof. Batu Erman

ABSTRACT

Key Words: T Cell, Thymocyte Development, Somatic V(D)J Recombination, DNA Damage Response, Patz1/MAZR, p53, co-Immunoprecipitation, Homology Modeling, Apoptosis

T lymphocytes make up an important line of defense against invading pathogens and tumors, where the success of the immune response depends on the range of threats that can be identified properly. The diversity required for the antigen-specific T cell receptors (TCRs) is achieved through a biological mechanism called somatic V(D)J recombination, where double-stranded DNA breaks naturally occur as a result of gene rearrangements in the TCR gene loci during T cell development. The process is tightly regulated by the tumour suppressor p53 through the activation of several DNA damage checkpoints.

To investigate how p53 controls T lymphocyte developmental checkpoints we studied its interaction with transcription factors known to be expressed in developing T cells. Using computer-stimulated computer modeling backed up by co-immunoprecipitation studies, we showed that Patz1/MAZR interacts with the basic C-terminal domain of p53 through an isoform 001-specific binding pocket generated by the 6th and the 7th C_2H_2-type zinc finger motifs that is not present in other alternatively spliced Patz1/MAZR isoforms. Furthermore, we demonstrated that residues Asp521

and Asp527 located in the binding pocket play a critical role for the interaction of p53 by site-directed mutagenesis. Cell survival assays performed in the immortalized human cell line HEK293T and DP mouse lymphoma cell lines AKR1 and VL3 showed that the Patz1/p53 interaction confers protection against cell death and inhibits p53-induced apoptosis.

T HÜCRESİ GELİŞİMİ SIRASINDA

BTB/ZİNC FİNGER TRANSKRİPSİYON FAKTÖRÜ PATZ1/MAZR'IN

P53 REGÜLASYONLU DNA HASARINA TEPKİ

MEKANİZMASINDAKİ ROLÜ

Manolya Ün

Yüksek Lisans Tezi 2011

Tez Danışmanı: Assoc. Prof. Batu Erman

ÖZET

Anahtar Kelimeler: T Hücresi, Timosit Gelişimi, Somatik V(D)J rekombinasyonu, DNA hasarına tepki, Patz1/MAZR, p53, İmmün çöktürme, Homoloji Modellenmesi, Apoptoz

T lenfositler, patojenlere ve kanserli hücrelere karşı oluşturulan savunma hattının önemli parçalarıdır. Bu gibi tehditlere karşı verilen immün tepkinin başarısı, doğru olarak tanımlanabilen tehdit sayısıyla orantılı olduğundan antijen-spesifik T hücresi algaçları geniş bir çeşitlilik aralığına sahip olmalıdır. Gereken çeşitlilik somatik V(D)J rekombinasyonu olarak bilinen süreç sonunda çift zincirli DNA'nın kırılması ve T hücresi reseptörünü kodlayan genomik bölgenin yeniden düzenlenmesi ile sağlanır. Somatik V(D)J rekombinasyonunun tümör baskılayıcı p53 tarafından aktive edilen DNA hasar-kontrol noktalarınca regüle edildiği bilinmektedir.

Bu çalışmada BTB-POZ/Zinc Finger bölgeli bir transkripsiyon faktörü olan Patz1/MAZR'ın somatik rekombinasyon tarafından tetiklenen p53 regülasyonlu DNA

hasarına tepki yolağında etkili olduğunu gösterdik. Araştırmamızda bilgisayar ortamında simule edilmiş homoloji modellerinden ve immün çökeltme deneylerinden yararlanarak Patz1/MAZR'ın p53'e C-terminal bölgesinden bağlandığını ve bu etkileşimin MAZR001 protein isoformuna spesifik bir bağlanma cebi tarafından kurulduğunu gösterdik. Homoloji modeli bağlanma cebinin 6. ve 7. zinc finger bölgelerinin arasında bulunduğunu ve diğer isoformlarda böyle bir yapıya rastlanmadığını ortaya koydu. Bunun yanısıra bağlanma cebinde bulunan Asp521 ve Asp527 amino asitlerinin Patz1/MAZR-p53 etkileşiminde kritik bir rol üstlendiğini proteinde kontrollü nokta mutasyonları yaparak gösterdik. İnsan hücre hattı HEK293T ve çifte pozitif fare lenfoma hatları AKR1 ve VL3 üzerinde yapılan hayatta kalma deneyleri, bu etkileşimin p53 tarafından indüklenen apoptozu baskılayarak hücreleri ölümden koruduğunu ortaya çıkardı.

FOR MY EXTENDED FAMILY...

ACKNOWLEDGEMENTS

TABLE OF CONTENTS

LIST OF FIGURES

LIST OF TABLES

THE LIST OF ABBREVIATIONS

α	Alpha
β	Beta
γ	Gamma
7AAD	7-aminoactinomycin D
ADR	Adriamycin
Amp	Ampicillin
APS	Ammoniumpersulfate
Asp	Aspartic Acid
ATM	Ataxia Telangiectasia Mutated
ATP	Adenosine Triphosphate
bps	Basepairs
Bcl6	B Cell Lymphoma 6 Protein
BSA	Bovine Serum Albumine
BTB	Broad Complex/Tramtrack/Bric-a-Brac
CaCl$_2$	Calcium Chloride
cDNA	Complementary DNA
CIAP	Calf Intestinal Alkaline Phosphatase
CJ	Coding Joint
co-IP	co-Immunoprecipitation
D	Aspartic Acid
DBD	DNA-binding Domain
DDR	DNA Damage Response
DMEM	Dulbecco's Modified Eagle Medium
DMSO	Dimethylsulfoxide
DN	Double Negative
DNA	Deoxyribonucleic Acid
DP	Double Positive
dsDB	Double-stranded DNA break
EDTA	Ethylenediaminetetraaceticacid
E8	CD8 Enhancer Element

ETP	Early Thymocyte Progenitor
FACS	Fluorescence Activated Cell Sorting
FBS	Fetal Bovine Serum
FIT-C	Fluorescein Isothiocyanate
GC	Germinal Center
HDAC	Histone Deacetylase
HEK	Human Embryonic Kidney
HBS	HEPES-buffered Saline
HRP	Horseradish Peroxidase
HSC	Hematopoietic Stem Cell
IL	Interleukin
LB	Luria Broth
Lys	Lysine
K	Lysine
MAZR	MAZ-related Factor
MHC	Major Histocompatibility Complex
NHEJR	Non-homologous End-Joining Repair
NLS	Nuclear Localization Signal
OD	Optical Density
PBS	Phosphate Buffered Saline
PCR	Polymerase Chain Reaction
PK	Protein Kinase
PNK	Polynucleotide Kinase
POZ	Poxvirus and Zinc-Finger
pRD	Proline-rich Domain
RAG1	Recombination Activating Gene
RNA	Ribonucleic Acid
RNAi	RNA-interference
rpm	Revolution per Minute
RPMI	Roswell Park Memorial Institute Medium
SDS	Sodium Dodecyl Sulfate
Ser	Serine
TAD	Transactivating Domain

TBE	Tris-borate EDTA
TCR	T Cell Receptor
Tyr	Tyrosine
Y	Tyrosine
ZF	Zinc Finger

1   INTRODUCTION

1.1 T Cell Development in the Thymus

T cells are a type of white blood cells (lymphocytes) that are involved in the mediation of adaptive immunity in response to an antigen. The "T" in the name originates from "thymus", where bone marrow-derived precursors migrate to in the later phases of thymocyte maturation[1]. These stages of development have been characterized by the coordinated expression of T cell-specific surface markers such as the T cell receptor (TCR) complex and the co-receptors CD4 and CD8 (Figure 1.1):
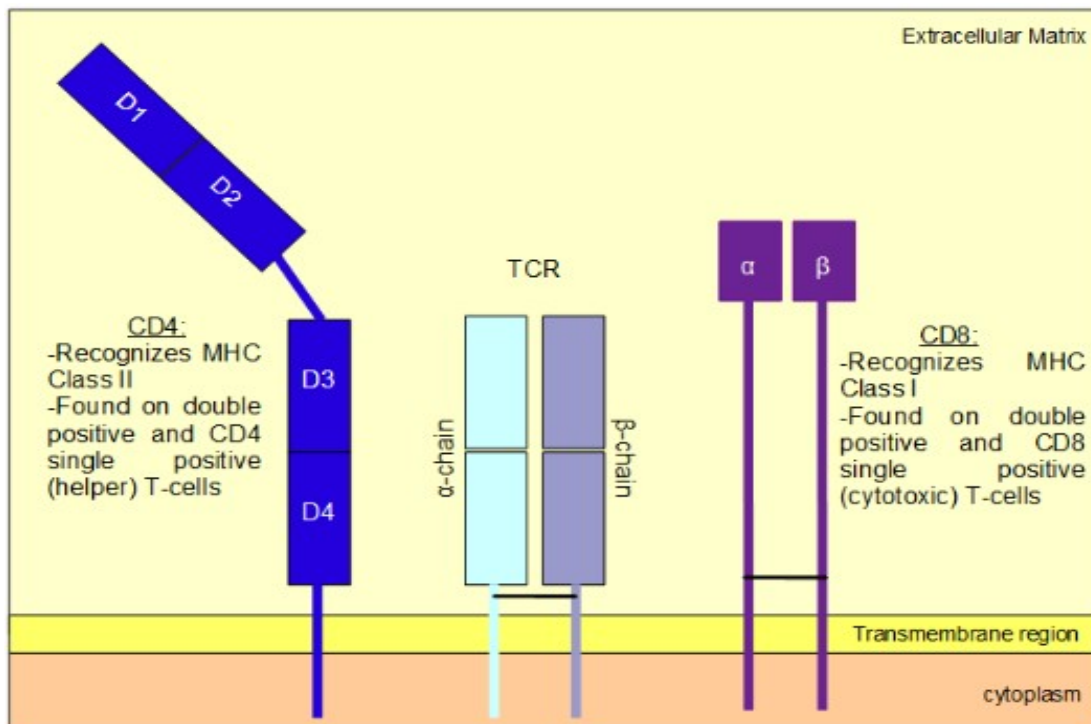
Figure 1.1: The major surface markers characterizing the stages of T-cell development in the thymus. The T cell receptor (TCR) complex consists of an α- (the green boxes) and a β-chain (lavender boxes). Its main function is to recognize antigenic peptide:MHC (major histocompatibility complex) complexes found on antigen-presenting cells and to activate mature T cells. The co-receptors CD4 (blue boxes) and CD8 (purple boxes), on the other hand, are expressed in a mutually-exclusive fashion on mature T cells. They participate in ligand binding and determine the sub-type of MHCs (major histocompatibility complexes) a given TCR can associate with.

T cell development in the thymus is a tightly regulated multi-step process, where several checkpoints exist to minimalize the maturation of cells with dysfunctional or self-reactive TCRs. In the initial stages, early thymocyte progenitors (ETPs) of hematopoietic stem cell origin leave the bone-marrow and home in the cortical regions of the thymus to differentiate into CD4(-)CD8(-) double-negative (DN) thymocytes that lack the said signature markers[2]. Such cells are devoid of a functional TCR complex, but begin to express the surrogate pre-TCRalpha chain along with the adhesion molecules CD44 and CD25 shortly after seeding the thymus[3]. The expression of pre-TCRalpha is followed by the recombinase activating gene (RAG)1/2-mediated rearrangement of the genomic TCRβ locus. This phenomenon is known as "somatic V(D)J recombination" and results in the production of a clone-specific TCR β-chain[4]. Among all DN thymocytes, only the ones that have successfully produced a functional β-chain can assemble a pre-TCR complex, proliferate and progress to the next stage of maturation.

The clones that have gone through a productive rearrangement migrate deeper into the cortical zones of the thymus and begin to differentiate into CD4 CD8 double-positive (DP) by simultaneously up-regulating the expression of the co-receptors. These cells subsequently undergo a second round of somatic recombination to rearrange the genomic TCRα locus. A productive rearrangement results in the generation of a clone-specific mature TCR complex containing both chains[5].

The success of somatic recombination, however, doesn't only depend on the proper assembly of a TCR. Since the process involves introducing double-stranded DNA breaks (dsDBs) and nucleotide additions/excisions to the target genomic loci, the introduction of mutations, deletions and insertions may prevent a fully-assembled TCR from associating with peptide:MHC (Major Histocompatibility Complex) conjugates or render it self-reactive[6]. In order to deal with this problem two powerful selection mechanisms are put to use:

During the first round of selection, also known as "positive selection", DP T cell clones in the thymus are trained by cortical epithelial cells that present self peptides in conjunction with MHCs. DP thymocytes with sufficiently active TCR complexes can

engage their ligands successfully and receive survival signals, whereas clones with nonfunctional TCRs die by apoptosis[7]. In the next step, positively-selected DP thymocytes are exposed to medullary epithelial cells or dendritic cells presenting self-peptide:MHC complexes. If the TCR:ligand association is too strong, implying an auto-reactive potential, the said clones are eliminated by apoptosis. This phenomenon is called "negative selection"[8].

Having survived the selective pressures in the thymus, DP thymocytes differentiate into a CD4(hi)CD8(lo) intermediate stage by down-regulating surface CD8 expression. This transient form has the potential to differentiate into either CD4 or CD8 single positive (SP) T cells[9]. Lineage commitment is thought to be orchestrated by the MHC specificity of the TCR complex: Canonically thymocytes with MHC-Class-I-specific TCRs turn into CD8 SP (cytotoxic) T cells, whereas those with MHC-Class-II-specific TCRs differentiate into CD4 SP (helper) T cells (Figure 1.2). Current models propose multiple mechanisms that might be involved in the determination of cell fate and several transcription factors are shown to regulate the process[10].
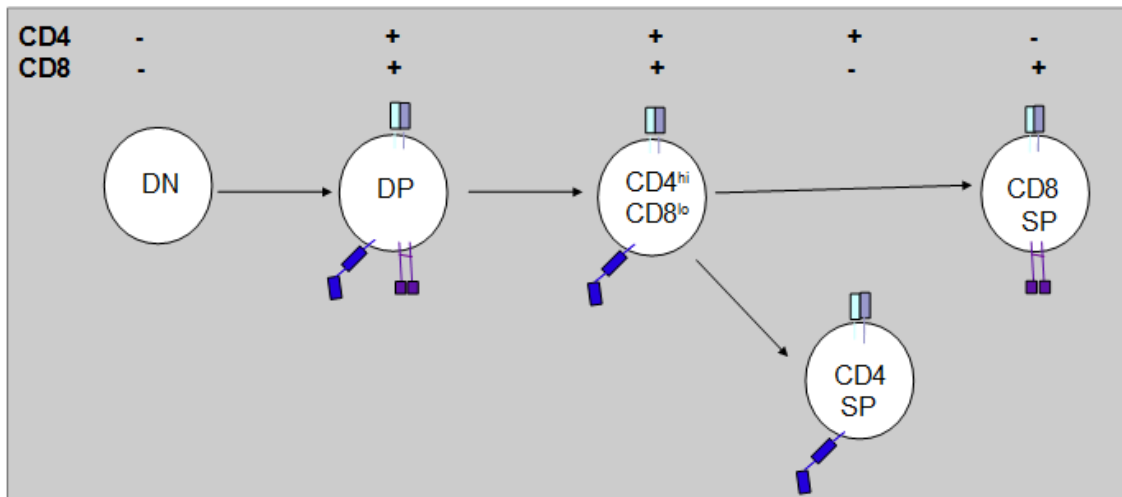
Figure 1.2: The stages of T cell development in the thymus in terms of TCR and co-receptor expression.
DN: Double negative, DP: Double positive, CD4(hi)CD8(lo): Intermediate, SP: Single positive. The TCR complex is indicated by the green-lavender boxes, CD4 by blue boxes and CD8 by purple boxes.

1.2 Somatic V(D)J Recombination: Mechanism

The goal of adaptive immunity is to recognize and eliminate foreign threats with the help of T and B lymphocytes during the later courses of infection. Since the induction of an efficient response is highly dependent on the range of threats that can be properly identified, the immune system must generate a vast repertoire of lymphocytes with unique receptors. To maintain such a level of diversity, T cells utilize combinations of a limited number of genomic segments to create countless numbers of clone-specific TCRs through a phenomenon called "V(D)J somatic recombination"[11]. The tightly regulated process introduces variations to the antigen-binding pockets of TCRs by randomly matching variable (V), diversity (D), and joining (J) gene segments and creating a joint V(D)J region flanking the constant region fragment to encode a TCR chain (Figure 1.3). Such a convoluted mechanism is required because an unlimited number of antigen-specific receptors can't be encoded by the genome[12].
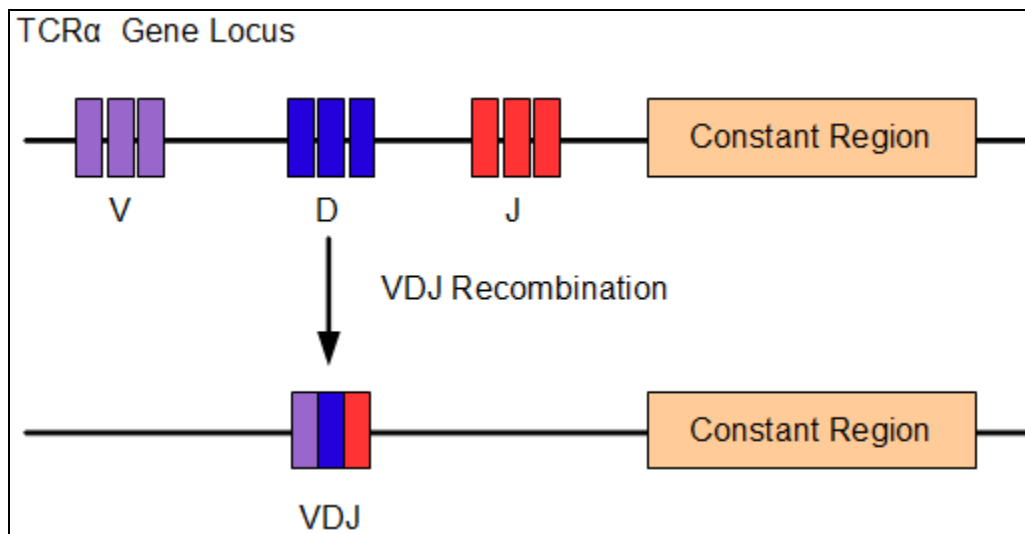
Figure 1.3: The rearrangement of the TCRα locus by V(D)J recombination in DP thymocytes. The V-segments are indicated by the purple boxes, D-segments by blue boxes, J-segments by red boxes and the constant region by the orange box. The diagram doesn't portray the number of the V-, D- or J-segments accurately.

The reaction begins with the generation of dsDBs in the recombination signal sites (RSS) (a conserved nonamer and heptamer sequence separated by a 12- or 23 base-pairs-long spacer) flanking the segments to be joined by the RAG1/2 complex. During the later stages, the regions lying between the rearranged fragments are removed from the genome and the ends of the target segments are stuck together to generate "coding joints" (Cjs)[13,14]. The joining is mediated by the members of non-homologous end-joining repair (NHEJR) pathway such as DNA-PKs, Ku70/Ku80, Artemis, XRCC4, and DNA ligase IV. However, since the mode of action for the NHEJR pathway is far from being precise, CJs are hotspots for mutations, deletions and insertions[15].

1.3 The Induction of the DNA Damage Response (DDR) Pathway During Somatic Recombination

Although it's unlikely for a physiological event to induce significant DNA damage under normal conditions, the progression of V(D)J somatic recombination is, still, stringently regulated due to the risk of generating unrepaired dsDBs in highly proliferative DN and DP thymocytes (Figure 1.4).
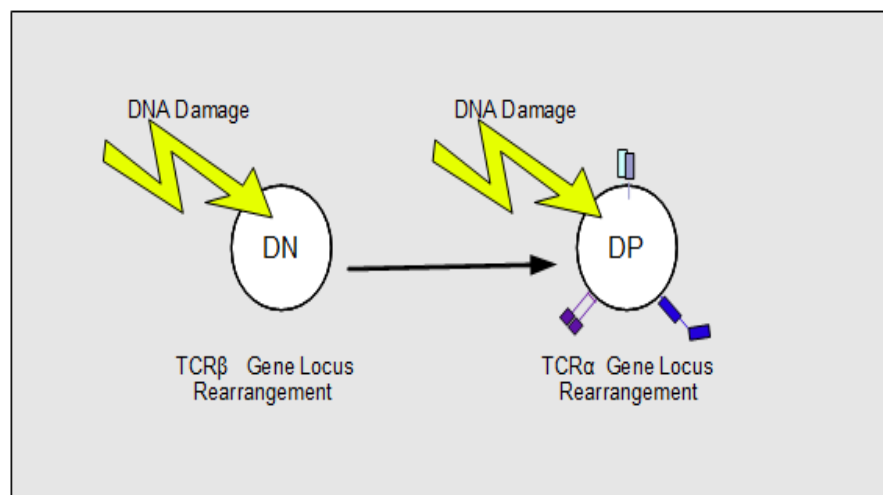
Figure 1.4: The rearrangement of the genomic TCR loci through V(D)J recombination generates dsDBs and induces DDR in DN and DP thymocytes during differentiation.
The TCR complex, the CD4- and the CD8 co-receptors on the DP thymocyte are depicted by the green-lavender, blue and purple boxes, respectively.

Control is exerted by restricting the recombinase activity of RAG1/2 to the non-cycling (G0/G1) stages of the cell cycle. Furthermore, RAG2 is swiftly phosphorylated and degraded before progression to the S phase occurs[16].

In addition to the coordinated regulation of somatic recombination and the cell cycle, the involvement of DDR pathway proteins in the larger picture has become another focus of interest. Recent studies report that ATM kinase deficiency leads to the persistence of dsDBs through the cell cycle in developing thymocytes[17-19] and the over-expression of p21 during G1 prevents the accumulation of RAG2[20]. In comparison to the other DDR pathway family members, however, the role of the tumor suppressor p53 in the progression of TCR loci rearrangement is probably the best documented, since it's one of the most rigorously studied in the fields of cell cycle control, cell death and cancer biology.

1.3.1 p53: Structure, Function and Regulation

The human gene TP53 is located at chromosome 17p13.1 and encodes the 393 amino-acids-long transcription factor p53 (Figure 1.5):
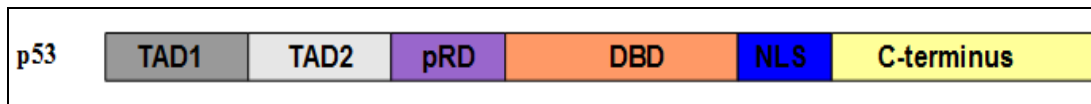
Figure 1.5: The structure of the full length human p53 protein. The protein is 393 amino-acids long, 53 kDa in size and consists of two conserved transactivation domains (TADs), a proline rich domain (prD), a DNA-binding domain (DBD), a nuclear localization signal (NLS) and a basic C-terminal domain.

The trans-activation domains (TADs) located at the N-terminus are responsible from mediating transcriptional activity and ubiquitination via Mdm2 binding, whereas the DNA-binding domain (DBD) in the center enables interactions with DNA in a sequence-specific manner. The proline-rich domain (pRD) spanning the region between the TADs and the DBD is reportedly required to support physical interactions with SH3-domain proteins[21]. Although its function is vastly unclear, the C-terminus of region of p53 flanking the nuclear localization signals (NLS) is thought to contain

ubiquitination sites for proteosomal degradation and may negatively regulate transcriptional activity by binding to unidentified repressors[22].

p53 exerts transcriptional activity in the form of a tetrameric body and is capable of both activating and repressing a large set of target genes[23,24]. Cellular stress is a potent inducer of the tumor suppressor function promoting either cell cycle arrest at G1and G2 phases or apoptosis according to the type and the intensity of the stressor. In the case of DNA damage, arrest is preferred and the expression of DNA-damage repair genes is up-regulated. If the damage is too grave and can't be salvaged, apoptosis is triggered to prevent further amplification of the genomic abnormalities. Mutations in p53 or other deficiencies in the down-stream apoptotic pathways are often the culprits for uncontrolled cell growth and carcinogenesis[25-27].

One of the most thoroughly-studied transcriptional targets of p53 is the cyclin-dependent kinase inhibitor p21 that is responsible from the induction of G1/G2 phase cell cycle arrest[28]. Other targets include the members of intrinsic and extrinsic apoptotic pathways such as Bax, PUMA, Caspase-6 and p53AIP1[21], DNA damage sensors XP-C and DDB2[29], and finally ubiquitin ligases MDM2 and Pirh2 that regulate p53 stabilization and degradation[30, 31]. In addition to its transcriptional activity, p53 is also shown to form inhibitory complexes with anti-apoptotic proteins Bcl2 and BclXL in the mitochondria through the DNA-binding domain and promote the release of cytochrome c into the cytoplasm during apoptosis[32].

In the absence of cellular stress, p53 levels in a cell are undetectable or low owing to a half-life of 10-20 minutes depending on the cell type[21]. The rapid proteasomal degradation is a result of ubiquitination by Mdm2, Pirh2 and p300 at the TADs or DBD of p53[30, 31]. Exposure to stressors, on the other hand, tend to stabilize p53 by inducing a number of kinases such as ATM, ATR, Chk2 and DNA-PK that phosphorylate the tumor suppressor at a number of Ser/Thr residues[33-35]. It has been reported that phosphorylation patterns are stressor-specific and may influence the outcome of the cell fate decision differentially by modifying transcriptional target selectivity. As an example, exposure to genotoxic drugs cisplatin and camptothecin favors the phosphorylation of Ser15 alone, whereas ionizing radiation tends to increase

phosphorylation at Ser6 and Ser9 as well[36, 37].

1.3.2 The Role of p53 in Somatic V(D)J Recombination

Induced upon genotoxic stress, p53 is an ideal candidate to regulate the progression of developing thymocytes through DNA damage checkpoints during somatic recombination. The critical role of p53 in this regard was first demonstrated in RAG2-/- mice that showed a severe-combined-immune-deficient-(SCID)-like phenotype. The thymocytes from RAG2-/- mice are arrested at the early DN stage of development since they can't undergo a successful rearrangement of the TCRβ GENE locus. The existing under-developed thymocytes are also reported to have a short lifespan due to the lack of surface TCRbeta signaling, which is thought to suppress the dominant apoptotic pathway regulating the recombination process[38]. A critical study in the field has shown that sublethal doses of γ-irradiation could relieve the SCID-like phenotype and allow DN cells to progress to the DP stage of development without the requirement for productive TCRβ locus rearrangement or surface TCR expression. The radiation-induced mutations responsible for the TCR(-) DP thymocyte phenotype were mapped to the p53 gene locus implying the loss of p53 function is sufficient for the progression from the DN to the DP stage[39].

Interestingly, researchers working with p53-/- mice have failed to report any significant developmental abnormalities of the immune system, when the mice are grown under stress-free conditions. However, a previous study demonstrated that in (DNA ligase IV-/-)/(p53-/-) double knockout mice that have defective a NHEJR mechanism and lack the surface expression of a pre-TCRalpha complex due to failed genomic rearrangement, are more prone to generating spontaneous lymphomas, after exposure to UV-irradiation, in comparison to their DNA ligase IV-/- brethren[40]. Furthermore, it has recently been shown that dsDBs generated by somatic recombination tend to persist through the cell cycle in p53-/- and ATM-/- mice[19]. The fact that phosphorylated p53 has also been identified at actively rearranged V(D)J loci in complex with ATM implies that p53 might be one of the key regulators of somatic recombination (Figure 1.6)[41]:
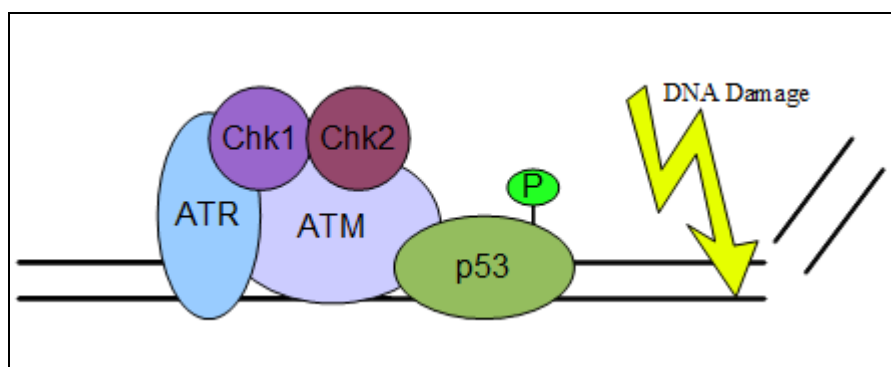
Figure 1.6: The co-localization of phosphorylated p53 at the dsDBs of actively rearranged TCR loci with the ATM:ATR complex during V(D)J recombination. The phosphorylated form of p53 (phosphorylation is indicated by the green "P" mark) is active and can induce apoptosis in response to genotoxic stress, if productive rearrangement can't be achieved.

1.4 The BTB/Zinc Finger Family of Transcription Factors

Transcription factors are the key mediators of tissue-specific and temporally-regulated gene expression. Owing to the modularity of their structural organization, such proteins can be classified based on the types of domains responsible for binding to DNA or interacting with other proteins or co-factors. According to these criteria, the BTB/zinc finger (BTB/ZF) family of transcription repressors can be characterized by the presence of a N-terminal POZ/Broad Complex, Tramtrack, and Bric à brac (BTB) domain and a varying number of C_2H_2-type zinc fingers located at the C-terminal. The evolutionarily conserved POZ/BTB domain enables homo- and heterodimerization, as well as protein–protein interactions, resulting in the recruitment of co-repressor complexes, whereas the zinc fingers are responsible for sequence-specific binding to DNA[42].

The physiological functions of BTB/ZF family proteins depend on the protein-protein interactions established through the BTB domain. Among such co-mediators, the co-repressors SIN3A, SMRT and NcoR1 are the most notable, which recruit HDACs (histone deacetylases) to the complex to induce deacetylation of histones in the local chromatin and keep the targeted genomic loci transcriptionally "silent"[43]. This

mechanism is thought to be the mode of action for BTB/ZF family-mediated gene repression (Figure 1.7):
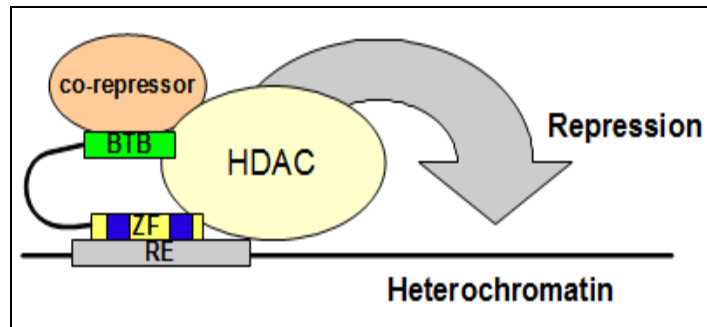
Figure 1.7: The induction of epigenetic silencing at a target genomic locus by a BTB/ZF family repressor. The transcription factor binds to the response element (RE) in the DNA via the zinc finger domain (ZF) and recruits a co-repressor with the help of the BTB domain. Finally a HDAC joins the repressor complex and induces the formation of transcriptionally silent heterochromatin through the deacetylation of local histones.

1.4.1 The Role of BTB/ZF Family in T Cell Development and Oncogenesis

Since BTB/ZF proteins serve as transcriptional switches that are able to open or close the target chromatin and epigenetically regulate gene expression from the afflicted locus, they are intensively studied in the context of cancer, stem cell and developmental biology[44]. Among the family members, 5 repressors with a highly conserved BTB domain have been shown to play a crucial role in T cell development and function. Some of these key players were also identified as proto-oncogenes[45].

The "T helper-inducing POZ-Krüppel factor" ThPOK, also known as c-Krox, is encoded by the human Zbtb7b gene and is expressed in CD4(hi)CD8(lo) intermediate and CD4 SP thymocytes[46]. Previous studies have shown that c-Krox promotes the generation of CD4 SP cells by preventing the Runx-dependent down-regulation of CD4 and repressing CD8 expression by blocking to the E81 CD8 enhancer[47]. It has been reported that a recessive mutation in gene is responsible for the generation of the "helper-deficient" phenotype in mice, where the differentiation of DP thymocytes to CD4 SP helper T cells is blocked. The diseased phenotype was rescued by

reconstituting the hematopoietic stem cell (HSC) pool with c-Krox[48, 49].

ROG/PLZP is encoded by the human Zbtb32 gene and is expressed in the thymus, spleen, lymph nodes and naive T cells. The expression in CD4 and CD8, however, is stimulated by TCR signaling[50]. PLZP is a negative regulator of interleukin-4 (IL-4) expression in CD8 SP T cells and mediates repression through the recruitment of HDAC complexes to the IL-4 promoter[51, 52]. The knockdown of the gene is reported to disrupt the homeostasis between quiescent and cycling subsets of HSCs and progenitor cells[53].

BCL6 is encoded by the human Bcl6 gene and the protein product was first characterized in a non-Hodgkin B cell lymphoma at a chromosomal break-point implying a role in oncogenesis[54]. The disruption of BCL expression in mice showed that the protein might be a key regulator of the adaptive immune response, since mutant mice failed to develop germinal centers required for B cells undergoing clonal expansion[55]. Recent studies also report that Bcl6 may be a negative regulator of B cell differentiation and prevent apoptosis in germinal centers. The protein has since been used as a common prognostic marker in patients with malignant forms of diffuse large cell lymphoma, where it's over-expressed[56, 57].

Although canonically considered as a culprit behind solid tumors such as melanomas and cervical tumors, BTB/ZF member PLZF was shown to interact with Bcl6 in vitro. The physical association is thought to mediate the recruitment of nuclear complexes involved in transcriptional silencing. Current studies focus on whether the PLZF/BCL6 interaction can be confirmed between endogenous proteins in non-Hodgkin lymphoma cell lines to determine the functional relevance[58].

Pokemon, encoded by the human gene Zbtb7 was first identified as a PLZP homologue that can bind to Bcl6 to increase its oncogenic potential and was used as another prognostic marker for lymphoma[59]. The disruption of Pokemon expression reportedly causes embryonic lethality due to anemia and dysregulation of cellular differentiation in various tissue types[60]. Additionally, Pokemon -/- mouse embryonic fibroblasts were shown to be resistant to oncogenic transformation, whereas transgenic

mouse models that over-expressed the gene in immature T and B cells developed spontaneous tumors through the down-regulation of p53[61].

1.4.2 Patz1/MAZR

The MAZ-related factor Patz1/MAZR, encoded by the human gene Zfp278, is a BTB/ZF family transcription factor that is predominantly expressed in the brain, skin, testicular tissues and thymus. It was first identified as a novel zinc finger gene fused to EWS in Ewing sarcoma[62] and was later shown to interact with RNF4 to mediate the transcriptional repression of androgen receptor[63].

Patz1/MAZR has 4 known isoforms that are generated by alternative splicing. The widely-studied full length isoform MAZR001 has an N-terminal BTB domain that mediates protein-protein interactions and a C-terminal zinc finger domain consisting of 7 C_2H_2-type zinc fingers. The other isoforms share the BTB domain but differ in the number of individual zinc finger located in the C-terminus (Figure 1.8):
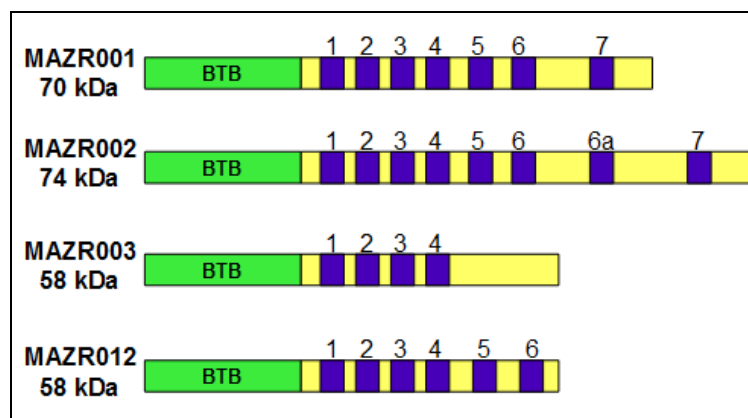
Figure 1.8: The protein structures of the alternatively-spliced Patz1/MAZR isoforms 001, 002, 003 and 012. Green box: BTB domain, Yellow box: Zinc finger domain Blue boxes: C_2H_2-type zinc fingers. Each zinc finger in a given isoform is assigned a number indicated above the blue boxes

The expression pattern of Patz1/MAZR is tightly regulated in developing T cells: The full length isoform MAZR001 is progressively down-regulated during the

transition from the DN to the DP stage, and is terminated once the assembly of a functional TCR is complete (Figure 1.9)[64]:
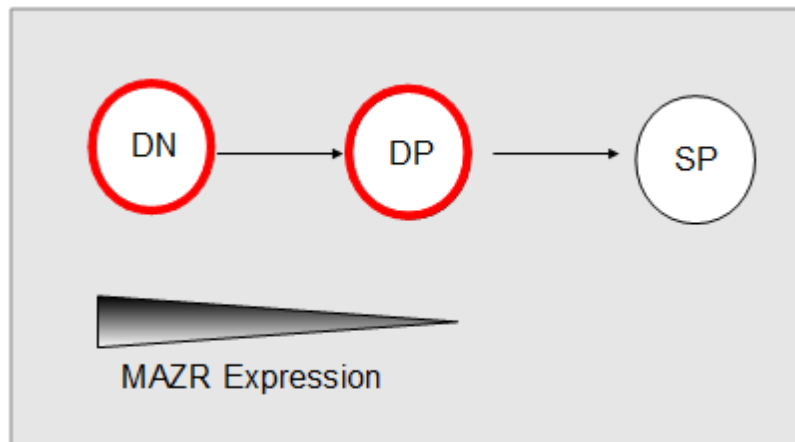
Figure 1.9: The expression pattern of Patz1/MAZR in developing T cells. MAZR is expressed in the double negative (DN) and to a lesser degree double positive (DP) stages of T cell maturation (phases marked by the red circles). Expression is terminated following the generation of a functional TCR in single positive (SP) stage.

In DN thymocytes MAZR001 is shown to interact with several CD8 cis-regulatory elements and induces epigenetic silencing of the locus by recruiting the nuclear co-repressor NcoR[64]. A recent study has demonstrated that the over-expression of MAZR001 induces variegated expression of CD8 in DP thymocytes highlighting a critical role in the CD4 vs. CD8 cell fate decision[65].

In addition to its involvement in the T-cell lineage commitment process, Patz1/MAZR over-expression has been identified as an underlying cause for colorectal[66] and testicular cancers[67], where the oncogenic effects are thought to be exerted by the upregulation of the proto-oncogene c-Myc.[68] The down-regulation of MAZR expression by RNA-interference (RNAi) is also reported to enhance the vulnerability of glioma cells to apoptotic stimuli highlighting a potential role in the regulation of cell cycle.[69]

During T cell development MAZR and the cell cycle regulator p53 are co-expressed in DN and DP thymocytes, when dsDBs physiologically occur as a result of somatic V(D)J recombination. The pair is, again, down-regulated following the

generation of a fully-assembled functional TCR (Figure 1.10)[70]:
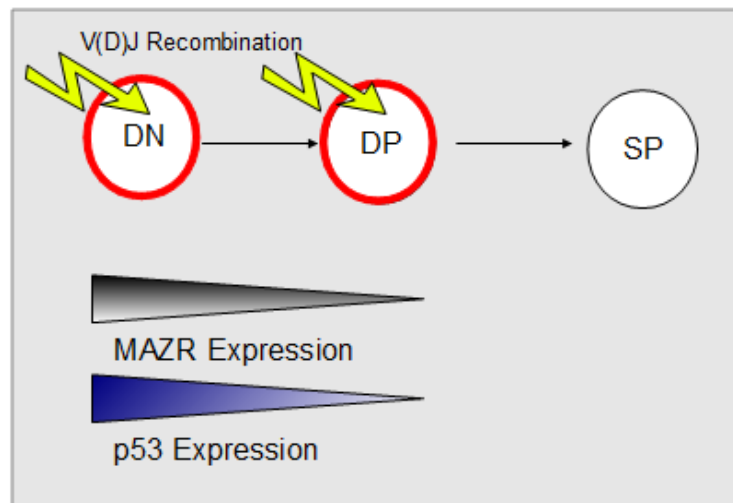
Figure 1.10: The coordinated expression pattern of Patz1/MAZR and p53 during T cell development. Both proteins are expressed at double negative (DN) and double positive (DP) stages, where DNA damage (indicated by the lightning sign) occurs due to somatic recombination. Once the rearrangement of the TCR locus is completed in single positive (SP) cells, the genes are progressively down-regulated.

The coordinated expression patterns with p53 may imply that MAZR, like other proto-oncogenic BTB/ZF family members, may participate in the p53-mediated regulation of DNA damage response during somatic recombination.

2 AIM OF THE STUDY

BTB/Zinc finger (BTB/ZF) transcription factor family proteins are critical mediators of T cell development and function. In addition to their role in T cell lineage commitment, some are reported to act as proto-oncogenes. The over-expression of these BTB/ZF family members have been observed in leukemias and lymphomas, where the oncogenic effects were shown to be exerted through the inhibition of p53-induced apoptotic pathways.

Our protein of interest, Patz1/MAZR, is a BTB/ZF repressor that is a negative regulator of surface co-receptor CD8 expression in double negative thymocytes. Aside from its involvement in cell fate decision, Patz1/MAZR was also identified as a putative proto-oncogene in colon cancer. The full length isoform MAZR001 and the master cell cycle regulator p53 are co-expressed in DN and double positive thymocytes, when double-stranded DNA breaks naturally occur as a result of somatic V(D)J recombination. The pair is, again, progressively down-regulated with the generation of a functional T cell receptor. The coordinated expression patterns with p53 and a possible role in oncogenesis lead us to investigate, whether Patz1/MAZR might be involved in the the regulation of the p53-induced DNA damage checkpoints during somatic V(D)J recombination.

The aim of this project was to investigate, whether Patz1/MAZR has a novel function in the p53-mediated steps of the DNA damage response during T cell development. By computational modeling and performing co-immunoprecipitation assays in the mammalian cell line HEK293T, we demonstrated that MAZR001 binds to the C-terminus of p53 through an isoform-specific binding pocket located in its zinc finger domain. We also identified Asp521 and Asp527 as the critical residues of the putative binding pocket responsible for the interaction through site-directed mutagenesis. Finally, cell survival assays performed in AKR1 and VL3 lymphoma cell lines demonstrated that the binding inhibited p53-induced apoptosis and implied that Patz1/MAZR is a potential proto-oncegene. Further elucidation of the mechanics behind this interaction can enhance our current understanding of the link between T cell development and lymphomagenesis.

3 MATERIALS AND METHODS

3.1 Materials

3.1.1 Antibodies, Chemicals and Media Components

The chemicals used in this study are listed below:

2-Mercaptoethanol (Sigma, Germany)

Acetic Acid (Merck, Germany)

Acrylamide/Bis-acrylamide (Sigma, Germany)

Adriamycin (Sigma, Germany)

Agarose (peQLab, Germany)

Ammonium Persulfate (Sigma, Germany)

Ampicillin Sodium Salt (Sigma, Germany)

Anti-c-Myc Agarose Affinity Gel Antibody (Sigma, Germany)

Anti-c-Myc Peroxidase, High Affinity (Roche, Germany)

Anti-FLAG Antibody (Sigma, Germany)

Anti-HA Agarose Affinity Gel Antibody (Sigma, Germany)

Anti-HA Peroxidase, High Affinity (Roche, Germany)

Anti-Histone H4K20monomethyl antibody (Abcam, England)

Anti-Histone H4K20dimethyl antibody (Abcam, England)

Anti-Histone H4K20trimethyl antibody (Abcam, England)

Anti-p53 Antibody (Cell Signaling Technology, USA)

Boric Acid (Molekula, UK)

Bradford Reagent (Biorad, USA)

Calcium Chloride (Merck, Germany)

Cisplatin (Kocak Farma Ilac, Turkey)

DDT (Fermentas, USA)

DMEM (Invitrogen, USA)

DMSO (Sigma, Germany)

DNA Loading Dye (Quality Biological Inc., USA)

EDTA (Applichem, Germany)

Ethanol (Sigma, Germany)

Ethidium Bromide (Merck, Germany)

Fetal Bovine Serum (FBS) (Biological Industries, Israel)

Glycerol (Riedel-de Haen, Germany)

HEPES (AppliChem, Germany)

Hydrochloric Acid (Merck, Germany)

Isopropanol (Riedel-de Haen, Germany)

L-glutamine (Hyclone, Germany)

Liquid Nitrogen (Karbogaz,Turkey)

Lumi-Film Chemiluminescent Detection Film (Roche, Germany)

Luria agar (Difco, USA)

Luria Broth (Difco, USA)

Magnesium Chloride (Promega, USA)

Methanol (Sigma, Germany)

Penicillin-Streptomycin (Biological Industries, Israel)

Phenol-Chloroform-Isoamylalcohol (Amersco, USA)

PIPES (Sigma, Germany)

Potassium Chloride (Fluka,Switzerland)

Potassium Hydroxide (Merck, Germany)

Protease Inhibitor Tablets (EDTA-free) (Roche, Germany)

ProteinA-HRP (Sigma, Germany)

ProteinA Sepharose Beads (Amersco, USA)

ProteinG Sepharose Beads (Amersco, USA)

ProteinG-HRP (Sigma, Germany)

PVDF Membrane (Millipore, USA)

RNAse A (Roche, Germany)

RPMI (without L-Glutamine) (Invitrogen, USA)

Sodium Dodecyl-Sulfate (Applichem, Germany)

SDS Protein Loading Dye (Fermentas, USA)

Sodium Chloride (AppliChem,Germany

Sodium Hydroxide (Merck, Germany)

Skim Milk Powder (Fluka, Germany)

Sodium Azide (Amersco, USA)

Sodium Chloride (Applichem, Germany)

TEMED (Applichem, Germany)

Tris Base (Amersco, USA)

Tris Hydrochloride (Amersco, USA)

Triton-X 100 (Promega, USA)

Tween20 (Sigma, Germany)

Supersignal West Pico Chemiluminescent Substrate (Thermoscientific, USA)

Trypan Blue (Sigma, Germany)

Trypsin-EDTA (Biological Industries, Israel)

3.1.2 Equipment

The equipments used in this study are listed below:

Autoclave (Hirayama, Hiclave HV-110, Japan)

Bacterial Incubator (Memmert, Model 300, Germany; Memmert Model 600, Germany)

Cell Counter (Cole Parmer, USA)

Centrifuge (Eppendorf, 5415D, Germany; Hitachi, Sorvall RC5C Plus, USA)

CO_2 Incubator (Binder, Germany)

Deepfreeze (Forma, Thermo ElectronCorp., -80 degrees C, USA; Bosch, -20 degrees C, Turkey)

Distillator (Millipore, Elix-S, USA)

Electroporator (Invitrogen, Neon Transfection Systems, USA)

Electrophoresis Apparatus (Biogen Inc., USA; Biorad Inc., USA)

Filter Membranes (Millipore, USA)

Flow Cytometer (BDFACS Canto, USA)

Gel Documentation (Biorad, UV-Transilluminator 2000, USA)

Heater (Eppendorf, Thermomixer Comfort, Germany)

Hematocytometer (Hausser Scientific, Bluebell Pa., USA)

Ice Machine (Scotsman Inc., AF20, USA)

Laminar Flow (Heraeus, HeraSafe HS12, Germany)

Liquid Nitrogen Tank (Taylor-Wharton, 3000RS, USA)

Magnetic Stirrer (VELP Scientifica, ARE Heating Magnetic Stirrer, Italy)

Micropipettes (Gilson, Pipetman, France)

Microwave Oven (Bosch, Turkey)

pH meter (WTW, pH540 GLP MultiCal, Germany)

Power Supply (Biorad, PowerPac 300, USA)

Refrigerator (Bosch, Turkey)

Shaker (New Brunswick Sci., Innova 4330, USA)

PCR Thermocycler (Eppendorf, Mastercycler Gradient, Germany)

Vortex (Velp Scientifica, Italy)

3.1.3 Buffers and Solutions

Standard buffers and solutions used in this study were prepared according to the protocols in Sambrook et al., 2001[71].

Tris-Borate-EDTA (TBE) Buffer (1L, 10X):

104 g Tris-base

55 g Boric acid

40 ml EDTA (0.5 M, pH 8.0)

The solution is filtered and kept at room temeperature.

Agarose Gel (100 ml, 1% w/v):

1 g Agarose powder

100 ml TBE buffer (0.5 X)

The solution is boiled until clumps disappear. 0.01% (v/v) of ethidium bromide is added into the mix after cool-down.

Blocking Buffer (10 ml, 5% w/v):

0.5 g skim milk powder is dissolved in 10 ml 1X PBS.

Calcium Chloride Solution:

$CaCl_2$ (60 mM)

Glycerol (15% v/v)

PIPES (10 mM, pH 7)

The solution is autoclaved at 121 °C for 15 minutes and stored at 4 degrees C for competent cell preparation.

FACS Buffer (500 ml, 1X):

2.5 g Bovine serum albumine (BSA) (0.5% w/v)

0.5 g Sodium azide (0.1% w/v)

The solution is prepared in 500 ml of 1X PBS and stored at 4 degrees C.

Glycerol (200 ml, 90%):

180 ml of 100% Glycerol

The solution is autoclaved at 121 degrees C for 15 minutes and kept at room temperature under sterile conditions.

HEPES-buffered Saline (HBS) (100 ml, 2X, pH 7.05):

0.8 g NaCl

0.027 g $Na_2HPO_4.2H_2O$

1.2 g HEPES

The solution is filter-sterilized.

Phosphate-buffered Saline (PBS) (200 ml, 1X, pH 7.4):

1 tablet of PBS (P4417) is dissolved in 200 ml of deionized water to give 0.01 M phosphate buffer, 0.0027 M potassium chloride and 0.137 M sodium chloride. The solution should be filter-sterilized to be used in cell culture and is kept at room temperature.

PBS-Tween20 (PBST) (1L, 1X):

100 ml 10X PBS

2 ml Tween20

SDS Separating Gel (10 ml, 13%):

2.5 ml Tris 1.5M pH 8.8

4.34 ml Acryl:Bisacryl (30%)

100 ul 10% SDS

100 ul 10% APS

10 ul TEMED

SDS Stacking Gel (5 ml, 4%):

1.25 ml Tris 0.5M pH 6.8

1 ml Acryl:Bisacryl (30%)

50 ul 10% SDS

15 ul 10% APS

7.5 ul TEMED

SDS Running Buffer (1L, 10X):

30.3 g Tris-base

144 g Glycine

10 g SDS

Transfer Buffer (5L, 10X, pH 8.3):

1440 g Glycine

300 g Tris-base

Transfer Buffer (800 ml, 1X):

80 ml 10X Transfer buffer

160 ml Methanol

Trypan-Blue Dye (0.4% w/v):

40 g trypan-blue powder

10 ml PBS (1X)

The solution is stored at room temperature.

Triton-X 100 Lysis Buffer (10 ml):

0.5 ml 20% Triton-X 100

0.5 ml 1M Tris (pH 7.4)

0.3 ml 5M NaCl

1 tablet EDTA-free protease inhibitor

3.1.4 Growth Media

Luria Broth (LB) (1 L):

20 g LB powder

The solution is autoclaved at 121 °C for 15 minutes. Ampicillin is added to a final concentration of 100 ug/ml after cool-down for selection.

LB-Agar (1L):

20 g LB powder

15 g bacterial agar

The solution is autoclaved at 90 degrees C for 15 min. Ampicillin is added to a final concentration of 100 ug/ml after cool-down to ~40 degrees C for selection. The medium is then poured into sterile petri dishes, left to solidify at room temperature and subsequently kept at 4 degrees C.

Dulbecco's Modified Eagle's Medium (DMEM)

500 ml of commercial DMEM (without L-Glutamine)

Fetal bovine serum (FBS) (10% v/v)

L-Glutamine (2 mM)

Penicillin-Streptomycin (100 unit/ml each)

The medium is kept at 4 degrees C under sterile conditions and used to cultivate attached cell lines.

Roswell Park Memorial Institute Medium (RPMI):

500 ml of commercial RPMI (without L-Glutamine)

Fetal bovine serum (FBS) (10% v/v)

L-Glutamine (2 mM)

Penicillin-Streptomycin (100 unit/ml each)

2-mercaptoethanol (50 mM)

The medium is kept at 4 degrees C under sterile conditions and used to cultivate lymphoma cell lines.

3.1.5 Freezing and Storage Media:

Freezing Medium for Mammalian Cell Culture (50 ml, FBS: DMSO 9:1 v/v):

5 ml DMSO (sterile)

45 ml FBS (heat-inactivated)

The medium is kept at -20 degrees C under sterile condtions and warmed up to 4 degrees C prior to use.

Bacterial Glycerol Stocks (15% glycerol v/v):

834 μl of overnight-grown (16 hours, 270 rmp at 37 degrees C) bacterial LB culture

166 μl of 90% glycerol (15%, sterile)

The mixture is vortexed and stored at -80 degrees C in screw-cap tubes.

3.1.6 Molecular Biology Kits

Plasmid Midi Kit (QIAGEN)

Plasmid Maxi Kit (QIAGEN)

Phusion Site-directed Mutagenesis Kit (Finnzymes, Cat. No: F-541)

Qiaquick Gel Extraction Kit (QIAGEN)

3.1.7 Enzymes and Corresponding Reaction Buffers

The enzymes and their corresponding buffers used in this study are listed in Table 3.1 below:

Enzyme	Buffer	Source
CIAP	CIAP (10X)	Fermentas
EcoRI	EcoRI (10X)	Fermentas
Phusion Hot Start DNA Polymerase	Phusion HF (5X)	Finnzymes
PNK	Buffer A (10X)	Fermentas
T4 DNA Ligase	T4 (10X)	Fermentas
Quick T4 DNA Ligase	Quick Ligation Buffer (2X)	NEB

Table 3.1: The list of the enzymes and corresponding reaction buffers used in this study

3.1.8 Bacterial Strains and Mammalian Cell Lines

E. coli DH5-alpha (F- endA1 glnV44 thi-1 recA1 relA1 gyrA96 deoR nupG $!$ 80dlacZ″M15 ″(lacZYA-argF)U169, hsdR17(rK- mK+)) competent cells are used for plasmid amplification. Immortalized human cell line HEK293T and mouse lymphoma cell lines AKR1 and VL3 are used for transient protein expression.

3.1.9 Vectors and Primers

The vectors and primers used in this study are listed in Tables 3.2 and 3.3 below. The vector maps are provided in Appendix A.

Plasmid	Selection Marker	Purpose	Source
pCMV-HA	Ampicillin	Cloning	Clontech
pCMV-HA-MAZR	Ampicillin	Expression	Lab construct
pCMV-HA-MAZRAsp521Tyr	Ampicillin	Expression	Lab construct
pCMV-HA-MAZRAsp521/527Tyr	Ampicillin	Expression	Lab construct
pCMV-Myc	Ampicillin	Cloning	Clontech
pCMV-Myc-BTB	Ampicillin	Expression	Lab construct
pCMV-Myc-MAZR	Ampicillin	Expression	Lab construct
pFlag-CMV4	Ampicillin	Expression	Clontech
pFlag-CMV4-p53	Ampicillin	Expression	From Ozoren Lab, Bogazici University
SV40-p53	Ampicillin	Expression	From Bourdon Lab, Dundee University
SV40-p53	Ampicillin	Expression	From Bourdon Lab, Dundee University

Table 3.2: The list of the vectors used in this study

Primer	Sequence
MAZRAsp521Tyr (FWD)	5'-GACTCCTACGGTTACCTCTCCGACG-3'
MAZRAsp521Tyr (REV)	5'-GGAGCTCTCAATCAGATCCTGATGTG-3'
MAZRAsp521/527Tyr (FWD)	5'-TCCGACGCCAGCTACCTGAAGACG-3'
MAZRAsp521/527Tyr (REV)	5'-GAGGTAACCGTAGGAGTCGGAGCTCAC-3'

Table 3.3: The list of the primers used in this study and their sequences

3.1.10 DNA and Protein Molecular Weight Markers

DNA and protein molecular weight markers used in this study are listed in Appendix B.

3.1.11 DNA Sequencing

DNA sequencing was commercially performed by McLab, USA.

3.1.12 Software, Computer-based Programs and Websites

The software and online programs used in this project are listed below:

FinchTV   http://www.mclab.com

NCBI BLAST Server   http:/ncbi.nlm.nih.gov/blast.cgi

Immgen   http:/www.immgen.org

Prosite   http://prosite.expasy.org

Ensembl Genome Browser   http://www.ensembl.org

3.2 Methods

3.2.1 Vector Construction

Restriction Enzyme Digestion:

1 μg of target DNA was incubated with the restriction enzyme of choice and the corresponding buffer at 37 degrees C for 2 hours in a final volume of 20 μl. The products were either used for cloning or diagnostics.

Agarose Gel Electrophoresis and Gel Extraction of DNA:

1 g of agarose powder was dissolved in 100 ml of 0.5X TBE and the mixture was heated for 5 minutes in a microwave to yield a 1% (w:v) gel. Following cool-down to room temperature ethidium bromide was added to a final concentration of 0.001 (v:v). The gel was subsequently poured in the gel apparatus and left to polymerize. DNA samples (varying from 1 μl to 25 μl in volume) were mixed with 6X loading dye prior to loading.

Gels were run at 100 Volts for 90-110 minutes in 0.5X TBE and resulting band patterns were detected under UV light. Gel extraction of the bands was performed according to the guidelines provided with the QIAGEN Gel Extraction Kit.

Dephosphorylation of Vector Ends:

Digested vector ends were dephosphorylated by calf intestinal alkaline phosphotase (CIAP) at 37 degrees for 1 hour in the corresponding reaction buffer to prevent self-circularization of the empty vector during ligation. CIAP-treated samples were always gel-purified in advance of further processing.

Ligation:

The ligation of a DNA-insert to a vector backbone was carried out using a 1:3 vector:insert ratio. Reactions were performed at 4 degrees C overnight (16 hours) in a final volume of 20 μl using T4 DNA ligase and the corresponding buffer. The ligation products were either stored at -20 degrees C or used to transform chemically competent E. coli.

3.2.2 Bacterial Cell Culture

<u>Culture Growth and Preparation of Glycerol Stocks:</u>

Liquid cultures were grown in appropriate amounts of LB (antibiotics optional) at 37 degrees C overnight (16 hours) shaking at a rate of 270 rpm. To obtain single colonies, cells were spread LB agar dishes and grown at 37 degrees C overnight. To prepare glycerol stocks for long-term storage, 90% glycerol was mixed with sufficient amounts of overnight liquid cultures to give a final concentration of 15% in ~ 1 ml. Glycerol stocks were stored in screw-cap tubes and kept at -80 degrees C.

<u>Competent Cell Preparation:</u>

A single colony from previously prepared competent E. coli DH5-alpha was picked from the surface of an LB-agar medium without selective antibiotics to serve as the starter. The starter colony was grown in a volume of 50 ml LB without antibiotics at 37 degrees C overnight at 270 rpm. On the following day, 4 ml from the overnight culture transferred into 400 ml of fresh LB and inoculated under the same growth conditions until the optical density of the medium at 590 nm (OD_{590}) was 0.375. In later steps, the bacterial cells were isolated and treated with CaCl2 solution multiple times to induce competency. Cells prepared this way were aliquoted in volumes of 100-200 μl and immediately frozen in liquid nitrogen to be stored at -80 degrees C for long-term use. The competency of the cells was affirmed by test transformations with varying concentrations of the plasmid pUC19 prior to use.

<u>Transformation of Competent Cells:</u>

Competent bacterial cells from -80 degrees C were thawed and incubated with 10-100 pg of target DNA for 30 minutes on ice. Following a heat-shock at 42 degrees C for 90 seconds, they were placed back on the ice to cool-down for 1 minute and subsequently incubated with fresh LB in a total volume of 1 ml for 45 minutes at 37 degrees C for recovery. Once transformed, the cells were streaked onto LB agar plates containing the appropriate antibiotics and grown at 37 degrees C overnight until single colonies become visible.

Plasmid Isolation:

Plasmid DNA isolation was carried out either by alkaline lysis for cloning purposes or according to the guidelines provided with the Midi- and Maxi-Prep Kits from QIAGEN to yield transfection-gradient DNA to use in mammalian cell culture. The starter cultures for both procedures were obtained from single colonies grown on LB agar dishes. The DNA-yield from the kits was quantified by Nanodrop.

3.2.3 Mammalian Cell Culture

Culture Growth and Preparation of Frozen Stocks:

The adherent cell line HEK293T was grown in sterile DMEM supplemented with heat-inactivated FBS (10%), L-Glutamine (2 mM), penicillin (100 unit/ml) and streptomycin (100 unit/ml). The suspension cell lines AKR1 and VL3 were kept in sterile RPMI supplemented with heat-inactivated FBS (10%), L-Glutamine (2 mM), beta-mercaptoethanol (50 mM), penicillin (100 unit/ml) and streptomycin (100 unit/ml). All cultures were maintained in a humidified incubator supplied with CO_2 (5%) at 37 degrees C and passaged into sub-cultures by 1:10 dilutions, once the cells reached ~80% confluency.

To prepare frozen stocks, cells at exponential growth phase were resuspended in freezing medium cooled to 4 degrees C and subsequently stored at -80 degrees C for 1 day to be transferred into the liquid nitrogen tank for long-term use. Freshly-thawed cells were washed with growth medium once to discard residual DMSO prior to the start of a new culture. Cells were frequently checked for abnormalities in morphology and growth rates under a light microscope. Cultures with high passage numbers were discarded.

Transfection:

A day prior to transfection, $5-10 \times 10^6$ HEK293T cells were seeded in 10-cm tissue culture plates and maintained under the standard tissue culture conditions described above. On the day of transfection, the growth medium of the target cells was refreshed 1 hour before the beginning of the procedure. 10 µg of plasmid DNA (in a

solution of 120 μl 1 M CaCl$_2$ and 500 μl of 2X HBS adjusted to 1 ml) was incubated at room temeperature for 10 minutes and delivered onto the cells via the "calcium-phosphate" (CaP) method. The medium containing the residual DNA:CaP complexes that weren't uptaken was removed and replaced by fresh media after 16 hours.

2x10^6 AKR1 cells were transfected with 10 μg of plasmid DNA in 100 ul of 1X HBS using a Neon Transfection Systems electroporator. DNA was delivered into the cells at 1400 V with a single pulse that lasted for 20 miliseconds.

10x10^6 VL3 cells were transfected with 10 μg of plasmid DNA in 100 ul of 1X HBS using a Neon Transfection Systems electroporator. DNA was delivered into the cells at 1500 V with a single pulse in 20 miliseconds.

Induction of DNA Damage Response:

HEK293T cells were treated with 30 μM of cisplatin for 24 hours, whereas AKR1 and VL3 lymphomas were treated with 1 μM of adriamycin for different time durations to induce DNA damage response.

Trypan-blue Exclusion:

HEK293T cells were washed with fresh culture medium and detached from the culture plate by vigorous pipetting. AKR1 and VL3 suspension cells were directly obtained from culture flasks. The cell suspension was diluted 1:1 in trypan-blue dye and 10 μl of the mixture was loaded on a hematocytometer. Live cell count was obtained by determining the number of unstained cells per compartment under a light microscope on 3 separate occasions and taking the average.

7AAD Staining and Flow Cytometry:

10^6 live (determined by trypan-blue exclusion) AKR1 or VL3 cells were precipitated by centrifugation at 1000 rpm for 5 minutes and washed three times with 1X FACS buffer. The suspensions were incubated with 1 μl of 7AAD (stock concentration 1 mg/ml) for 5 minutes at 4 degrees C in dark and analyzed by flow cytometry. The readings were obtained in the FIT-C channel.

Preparation of Whole Cell Lysates (WCLs):

36-48 hours after transfection, HEK293T cells were washed with ice-cold 1X PBS 3 times, transferred into a tube and lysed in 500-1000 μl of Triton-X 100 lysis buffer for 30 minutes on ice. The cell debris was precipitated by centrifugation at 4 degrees C for 15 minutes and the supernatant containing soluble proteins was transferred to a clean tube. The protein concentration of the WCL was determined by Bradford assay. The WCLs were either stored at -80 degrees for further analysis with Western blotting or immediately put to use for co-immunoprecipitation studies.

3.2.4. Protein-Protein Interaction Analysis

Co-Immunoprecipitation (Co-IP):

Co-IPs from HEK293T WCLs were performed with commercial anti-c-HA- or anti-Myc-antibody-conjugated agarose beads, anti-Flag (mouse monoclonal, Sigma), anti-Histone H4K20me1/2/3 (rabbit monoclonal, Abcam) and anti-p53 (rabbit polyclonal, Cell Signaling Technology) antibodies.

To prepare anti-Flag or anti-p53 beads, the corresponding antibodies were incubated with 30 μl of pre-washed agarose bead slurry at 4 degrees C overnight on a rotator (anti-Flag 1:200, anti-p53 1:500). The volume of the slurry is adjusted to 1 ml with 1X PBS to enable proper mixing. After washing 3 times with ice-cold PBS to get rid of the unbound antibodies, 1500 μg of WCL expressing the tagged proteins was mixed with the beads. The conjugation step was by-passed for the commercial anti-HA and anti-Myc beads.

After another round of incubation at 4 degrees C overnight on a rotator (in a volume of 1 ml adjusted with the lysis buffer), the beads were harvested by centrifugation at 12000 rpm for 30 seconds and washed 3 times with ice-cold lysis buffer. The resulting immuno-complexes were either kept at -80 degrees C or boiled in 5X protein loading dye (final concentration 2X in 30 μl) at 95 degrees C for 7 minutes for immediate analysis.

Western Blotting:

For protein gel electrophoresis, separating and stacking gels were prepared as described in "3.1 Materials". Prior to analysis 10-50 μg of WCL was boiled in 5X protein loading dye (final concentration 2X in 30 μl) at 95 degrees C for 7 minutes. 20-25 μl of the mixture was loaded per well in comparison to 5 μl of pre-stained protein marker (Fermentas) as molecular ladder.

Protein gels were run at 150-180V at room temperature in 1X running buffer prepared as described in "3.1 Materials". In contrast, the semi-dry transfer of proteins to a PVDF membrane was performed at 4 degrees C for at least 80 minutes at 100V. Coomassie-Blue staining was performed to affirm the success of transfer.

To detect the proteins of interest, the PVDF membrane was initially blocked in 5% milk-PBS for 1-2 hours at room temperature, washed 3 times with 1X PBST and later incubated at 4 degrees C overnight with the primary antibody of interest (anti-Flag 1:1000, anti-p53 1:2500) in 1% milk-PBS. In the case of anti-HA- and anti-c-Myc peroxidase incubation was performed at room temperature for 1 hour in 5% milk-PBS (each 1:1000). Following blotting with the relevant antibodies, the membrane was washed 3 times with 1X PBST and incubated with either proteinA-HRP (for anti-p53) or proteinG-HRP (for anti-Flag) each diluted by 1:10000 at room temeperature for 1 hour in 5% milk-PBS. This step was by-passed for anti-HA- and anti-c-Myc-HRP blots. After a final round of 3 washes with 1X PBST, the proteins of interest were visualized in the dark room with the application of a chemiluminescent substrate.

3.2.5 Site-directed Mutagenesis of Wild-type MAZR001

Introduction of Mutations by PCR:

A forward primer carrying the desired point mutation in the middle was designed to span the target site within MAZR001. The 5' end of the nonmutagenic reverse primer was chosen to complement the 5' end of the forward primer. The whole plasmid, pCMV-HA-MAZR, was used as the PCR template and the primer pair was used to generate a 5.8 kb-long linear product harboring the desired mutation. The

optimized PCR conditions are listed in Table 3.4 below:

Reagent	Volume	Final Concentration
pCMV-HA-MAZR (10 pg/μl)	5 μl	1 pg/μl
Phire Polymerase Buffer (10X)	10 μl	1X
dNTP Mix (10 mM)	1 μl	0.2 mM
Forward Primer (10 μM)	2.5 μl	0.5 μM
Reverse Primer (10 μM)	2.5 μl	0.5 μM
Phusion Polymerase (2 u/μl)	0.5 μl	0.02 u/μl
ddH$_2$O	28.5 μl	
Total	50 μl	

Table 3.4: The optimized PCR conditions for the
site-directed mutagenesis of wild-type MAZR001

The optimal thermal cycling conditions for PCR are as follows: Initial denaturation at 98 degrees C for 30 seconds, denaturation at 98 degrees C for 10 seconds, annealing at 60 degrees C for 20 seconds, extension at 72 degrees C for 5 minutes and final extension at 72 degrees for 5 minutes.

Phosphorylation of the PCR Products:

10 μg of isopropanol-precipitated PCR products were dissolved in 15 μl of ddH$_2$O and subjected to 5' end phosphorylation by polynucleotide kinase (PNK). The reaction was performed in a final volume of 20 ul in the corresponding buffer A supplemented with ATP (2 mM) at 37 degrees C for 30 minutes. The phosphorylated PCR products were agarose gel-purified according to the instructions provided with the QIAGEN Gel Extraction Kit.

Re-circularization of the PCR Products with Quick Ligation:

50 ng of phosphorylated PCR products were re-circularized by quick ligation in the corresponding quick ligase buffer in a final volume of 10 μl at room temperature for 5 minutes. The ligation products were immediately used to transform competent E. coli.

Selection of Point Mutants:

Competent E. coli transformed with the re-circularized plasmids were streaked on ampicillin-containing LB agar plates and grown overnight to obtain single colonies. Plasmid DNAs isolated from each single colony were sequenced to identify correct point mutants of MAZR001.

4   RESULTS

BTB/Zinc finger (BTB/ZF) transcription factor family proteins are critical mediators of T cell development and function[45]. Aside from their role in T cell lineage commitment, some may reportedly act as potential proto-oncogenes. The over-expression of these BTB/ZF family members have been observed in acute promyelocytic leukemias and non-Hogkin lymphomas[53, 56, 60] and the oncogenic effects were shown to be related to the inhibition of p53-induced apoptotic pathways[61, 72].

Patz1/MAZR, is a BTB/ZF transcriptional repressor that is a negative regulator of surface co-receptor CD8 expression in double negative (DN) thymocytes[65]. Aside from its involvement in cell fate decision, MAZR was also identified as a putative proto-oncogene in colon[66] and testicular cancer[67]. Interestingly, the full length isoform MAZR001 and the master cell cycle regulator p53 are co-expressed in DN and double positive (DP) thymocytes, when double-stranded DNA breaks (dsDBs) naturally occur as a result of somatic V(D)J recombination. The pair is, again, progressively down-regulated with the generation of a fully functional T cell receptor (TCR)[70]. The coordinated expression patterns with p53 and a possible role in oncogenesis lead us to investigate, whether Patz1/MAZR might have a novel function in the p53-regulated steps of the DNA damage response (DDR) during T cell maturation.

4.1 MAZR001 Interacts with DNA-damage-induced and ectopically-expressed p53 in HEK293T Cells

Recent studies report that some BTB/ZF family proto-oncogens can disrupt cell cycle by physically interacting with p53[73,74]. To test whether Patz1/MAZR has a similar property, we transfected HEK293T cells with either a Myc-BTB (the BTB domain of c-Krox, another member of the BTB/ZF family) or a Myc-MAZR (full length) expression vector. Following transfection, the cells were treated with 30 μM cisplatin for 24 hours to mount DDR and induce the expression of endogenous p53. Co-immunoprecipitation (co-IP) analysis showed that only full-length Patz1/MAZR, but not the BTB domain interacts with DNA-damage-induced p53 (Figure 4.1):
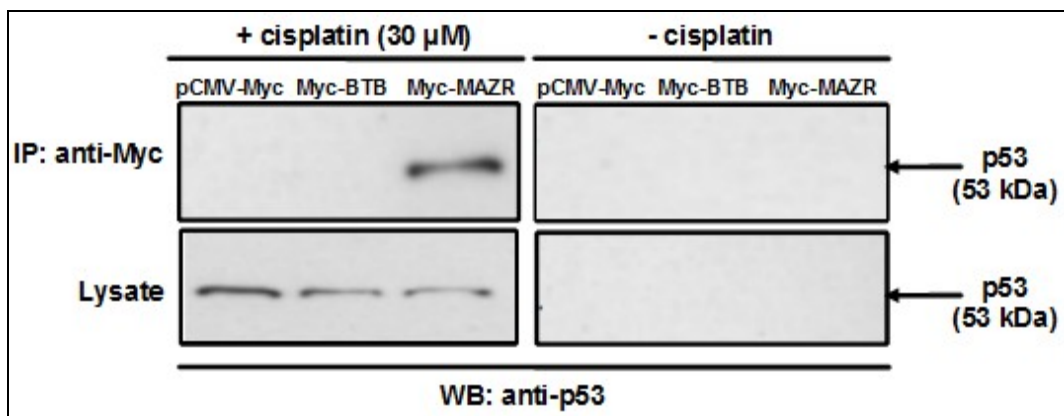
Figure 4.1: The co-IP of Myc-MAZR with cisplatin-induced endogenous p53 in HEK293T cells. On the left, whole cell lysates prepared from pCMV-Myc-, Myc-BTB- and Myc-MAZR-transfected and cisplatin-treated (30 μM, 24 hours) HEK293T cells were immunoprecipitated using anti-Myc antibodies. The immuno-complexes were analyzed by Western blotting using anti-p53 antibodies. On the right the whole cell lysates from untreated cells were immunoprecipitated using anti-Myc antibodies and blotted with anti-p53 antibodies to serve as a negative control.

The concentration of cisplatin used in the experiment above was taken from literature, whereas the duration of treatment was determined by a time-course study to obtain a significant rise in the levels of genotoxic-stress-induced p53 in HEK293T cells (Figure 4.2):
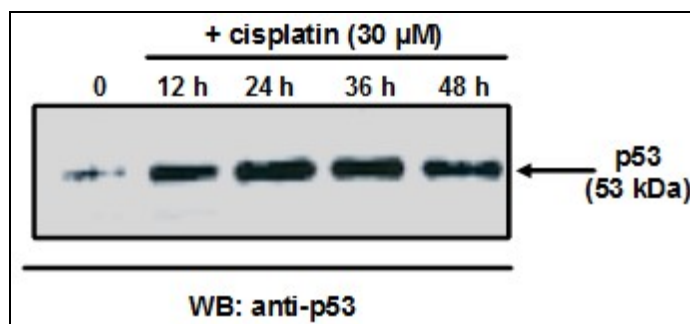
Figure 4.2: The time-course study conducted to find the optimal duration of cisplatin treatment for the upregulation of endogenous p53 expression in HEK293T cells. Whole cell lysates prepared from 30 μM cisplatin treated cells (for 12, 24, 36 and 48 hours respectively) were blotted with anti-p53 antibodies to detect the levels of stress-induced p53. Since p53 upregulation was sufficiently high after 24 hours in comparison to that of the untreated sample (0), the duration of treatment was restricted to a day. Each lane contains 10 μg of whole cell lysate.

In agreement with the data above, ectopically-expressed Flag-p53 could also be co-IPed with HA-MAZR from untreated HEK293T cell lysates. The physical interaction was demonstrated both ways (Figure 4.3):
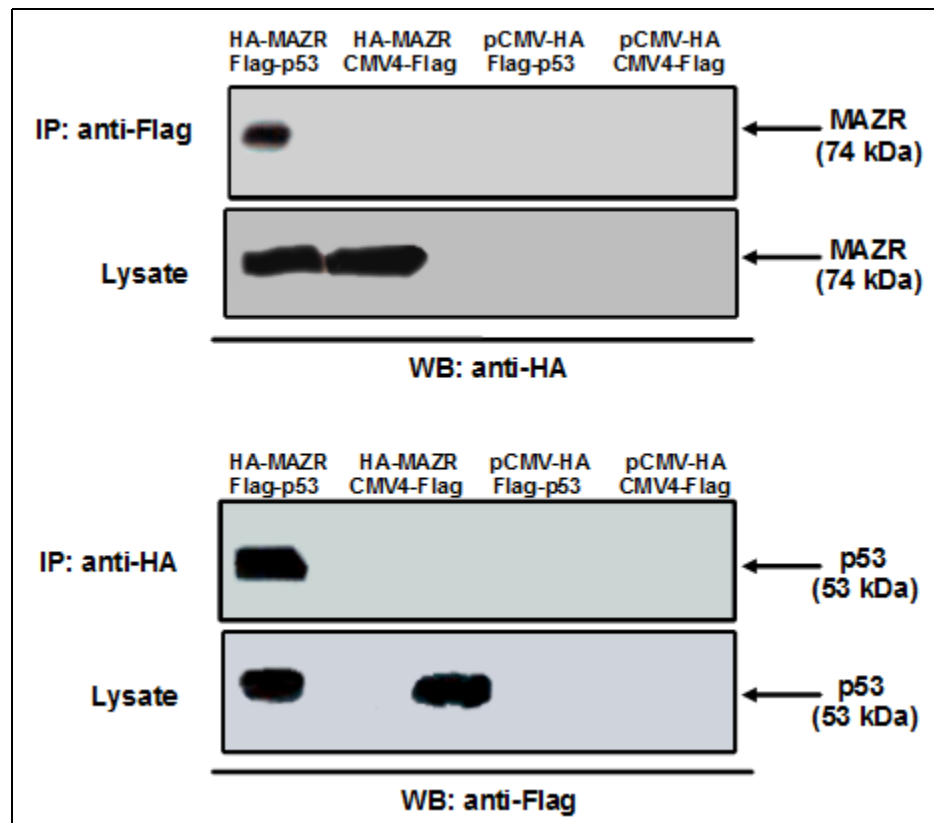
Figure 4.3: The co-IPs of ectopically-expressed HA-MAZR with Flag-p53 in HEK293T cells. On the upper panel **w**hole cell lysates were immunoprecipitated using anti-Flag antibodies and the immunocomplexes were analyzed by Western blotting using anti-HA antibodies. On the lower panel **w**hole cell lysates were immunoprecipitated using anti-HA antibodies and the immunocomplexes were analyzed by Western blotting using anti-Flag antibodies. 15 μg of whole cell lysate per lane (in the sub-panels captioned "Lysate") was used as input control.

The expression plasmid pCMV-HA-MAZR used in the co-IP assay above was constructed according to the following strategy (Figure 4.4).
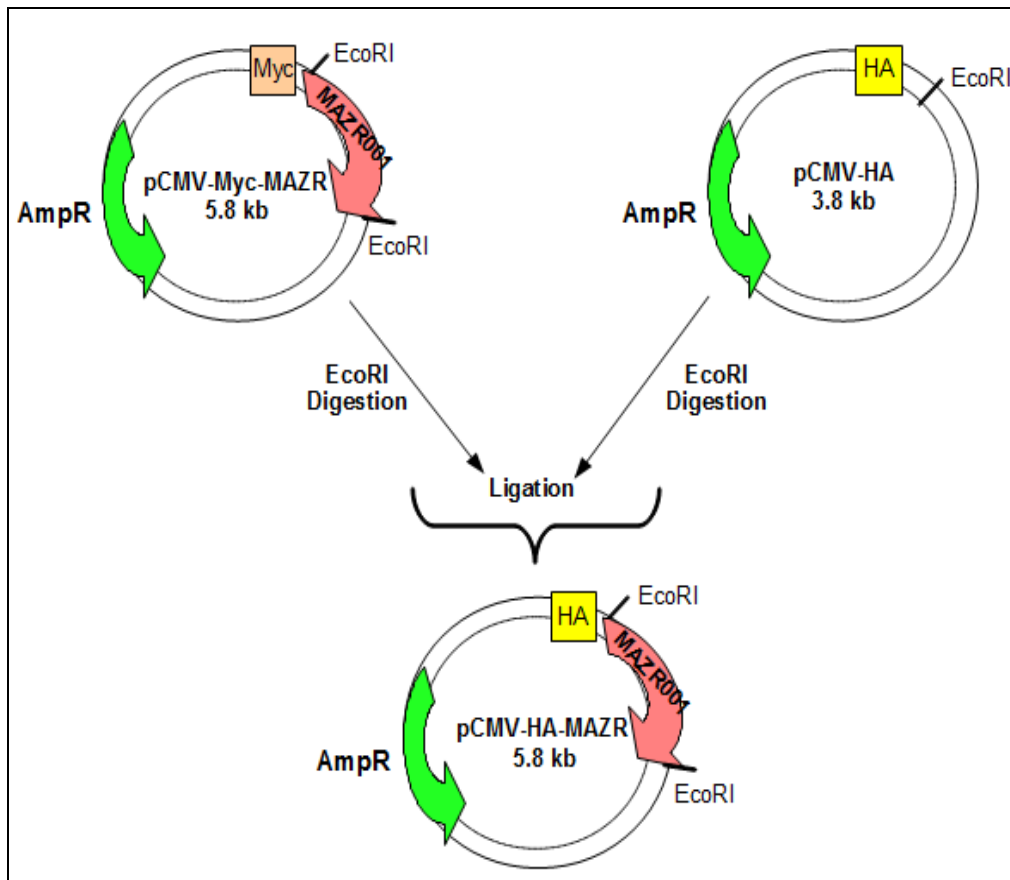
Figure 4.4: The cloning strategy for the construction of the mammalian expression plasmid pCMV-HA-MAZR. The cDNA fragment encoding mouse MAZR001 (~2000 bps-long, indicated by the pink arrow) was removed from the mammalian expression plasmid pCMV-Myc-MAZR by EcoRI digestion and ligated into the EcoRI-digested empty plasmid pCMV-HA (~3800 bps) to generate pCMV-HA-MAZR. The construct, which is 5.8 kb in size, contains a CMV promoter, an N-terminal HA-tag (HA indicated by the yellow box) and an ampicillin-resistance gene (AmpR indicated by the green arrow) as a bacterial selection marker.

Proper construction of the vector was confirmed by BamHI, EcoRI and XbaI diagnostic digests (Figure 4.5).
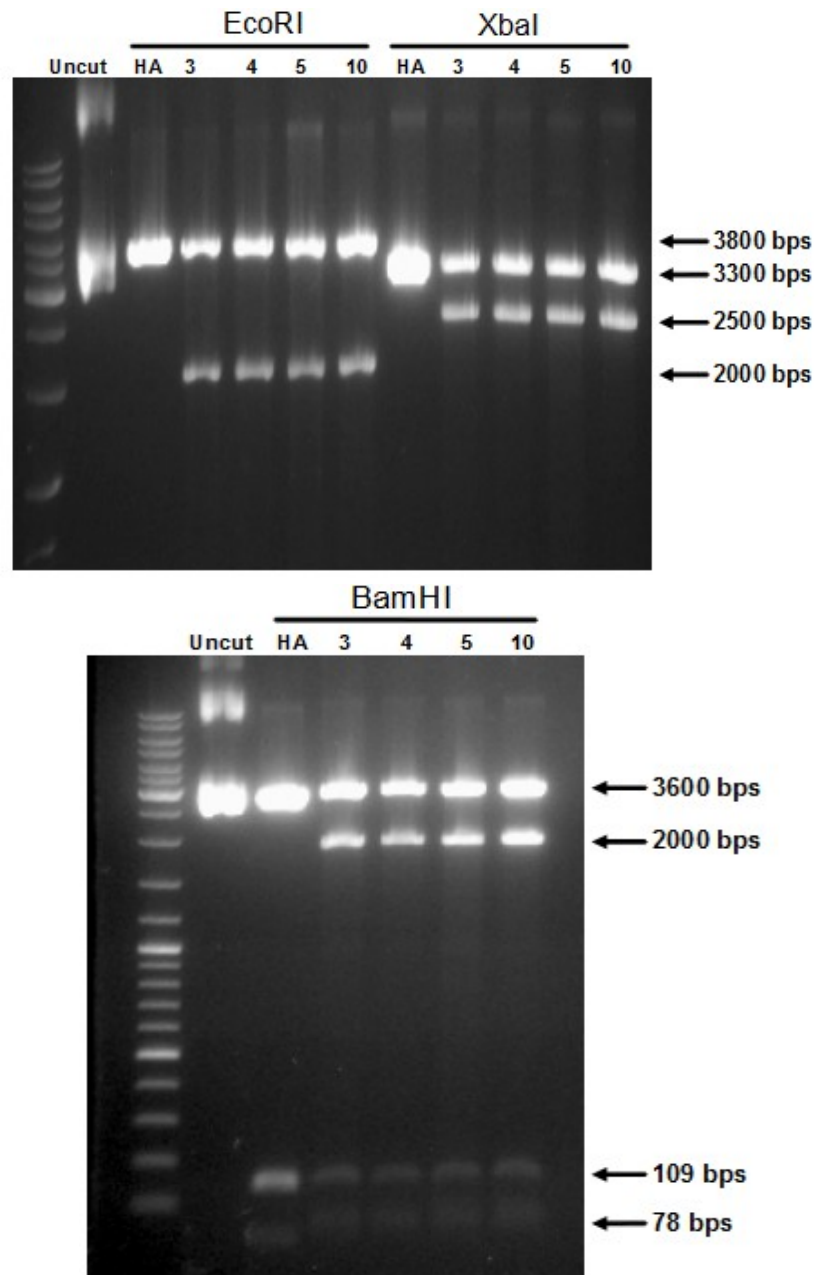
Figure 4.5: The diagnostic digests of pCMV-HA-MAZR with EcoRI, XbaI and BamHI. Upper Panel: The expected band lengths for the EcoRI digestion are 3000 and 2000 bps. For XbaI, they are 3300 and 2500 bps. Bottom Panel: The expected band lengths for the BamHI digestion are 3600, 2000, 109 and 78 bps. The numbering on top of the wells correspond to the identification number of the bacterial colony, from which the given plasmid has been isolated, whereas HA stands for the empty vector pCMV-HA run alongside the digestion products for control. Uncut denotes the undigested pCMV-HA expression plasmid. Each well contains 10 µl of the relevant digestion mix.

4.2 MAZR001 Interacts with the C-terminal Domain of p53

Having confirmed the physical association between Patz1/MAZR and p53, we set out to determine, which domains of p53 are necessary to support the interaction. The full-length protein isoform, known as p53-α, consists of 2 transactivation domains (TADs), a proline rich domain (prD), a DNA-binding domain (DBD), a nuclear localization signal (NLS) and a basic C-terminal domain, whereas a truncated isoform, called p53-β, lacks the latter (Figure 4.6)[75]. Although its function is widely unknown, current works imply that the C-terminus might be responsible from the regulation of p53 activity due to the presence of hotspots for post-translational modifications (PTMs)[22].
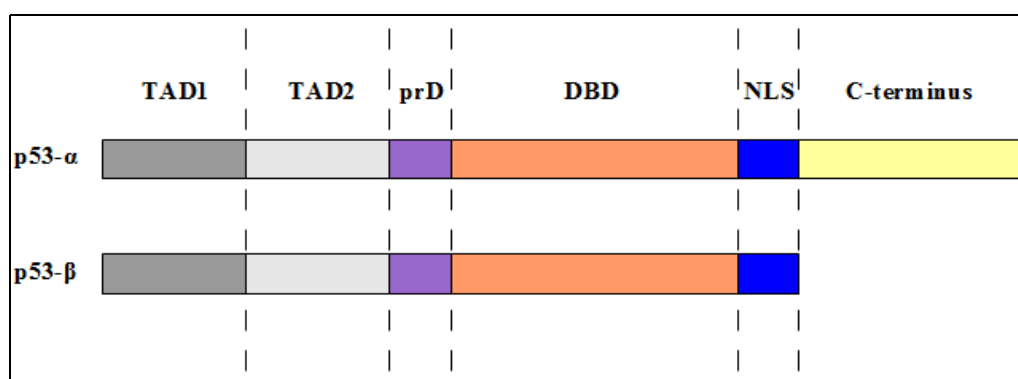
Figure 4.6: The protein structures of the human p53 isoforms, p53-α and p53-β. Both share conserved transactivation domains (TADs), a proline rich domain (prD), a DNA-binding domain (DBD) and a nuclear localization signal (NLS). The basic C-terminal domain, however, can only be found in the full-length isoform.

To determine, whether the basic C-terminus is involved in the physical interaction, we performed co-IPs using HEK293T whole cell lysates co-expressing HA-MAZR along with either p53-α or p53-β. Western blot analysis showed that Patz1/MAZR fails to interact with the truncated isoform p53-β suggesting the presence of the C-terminal domain is necessary to mediate binding (Figure 4.7):
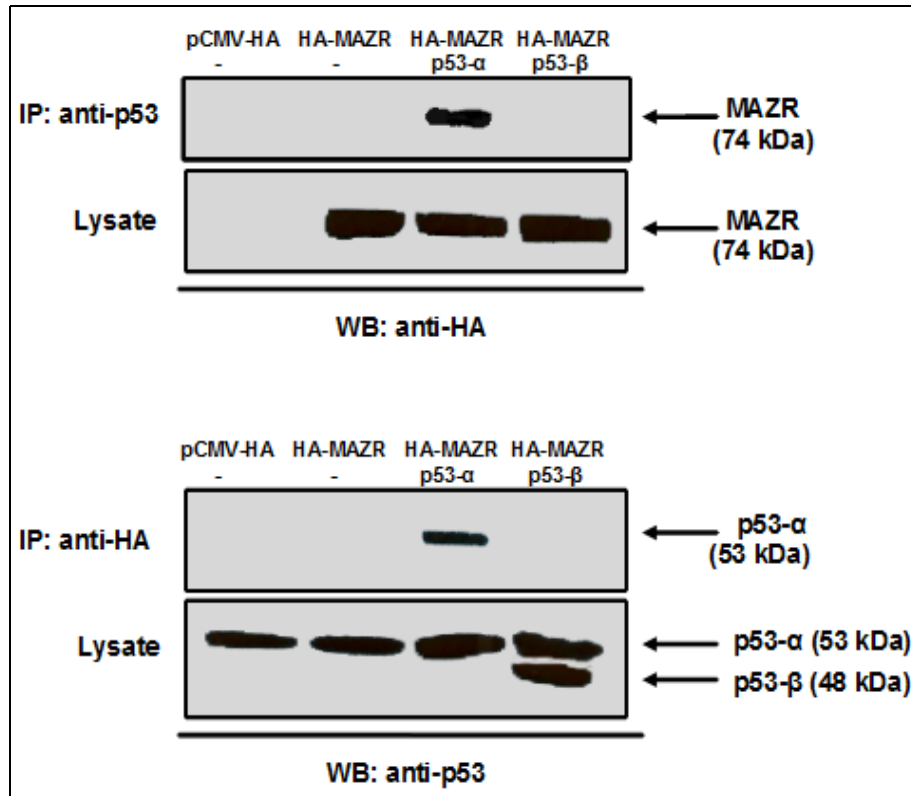
Figure 4.7: The co-IPs of ectopically-expressed HA-MAZR with p53-α and p53-β in HEK293T cells. On the upper panel whole cell lysates prepared from cells were immunoprecipitated using anti-HA antibodies and the immunocomplexes were analyzed by Western blotting using anti-p53 antibodies. On the lower panel whole cell lysates prepared from HEK293T cells were immunoprecipitated using anti-p53 antibodies and the immunocomplexes were analyzed by Western blotting using anti-HA antibodies. 15 μg of whole cell lysate per lane (in the sub-panels captioned as "Lysate") was used as input control.

4.3 MAZR001 Interacts with differentially-methylated
Forms of Histone H4K20

The C-terminal domain of p53 and the N-terminal tail of Histone H4 are reported to share a conserved "RHR/HK*" motif that is methylated at the lysine residue (K*) in response to DNA damage (Figure 4.8)[76]. The targeted lysine corresponds to K20 in Histone H4 and K382 in p53.

H4 1-24: SGRGKGGKGLGKGGAKRHRK*VL-R- - - -
p53 367-389: S - HLKS KKG - - -QSTSRHKK*LMFKTEG
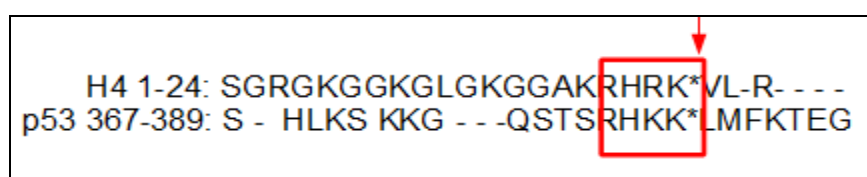
Figure 4.8: The protein sequence alignment of Histone H4 N-terminus (between amino acids 1 and 24) and p53 C-terminus (between amino acids 367 and 389). The homology region "RHR/HK" is indicated by the red frame. The asterix sign marking the last lysine residue in the motif (K*) indicates the location of methylation (also highlighted by the vertical red arrow). The methylation target corresponds to K20 in Histone H4 and K382 in p53.

The K20 residue of Histone H4 is a target of progressive methylation, where mono- and tri-methylation serve as hallmarks of epigenetic silencing, in contrast to di-methylation, which signals the mounting of DDR[77]. The K382 residue of p53, on the other hand, is reported to get mono-methylated, which results in the suppression of apoptotic activity[78] or di-methylated, which stabilizes p53 and increases the rate of accumulation upon DNA damage[79].

Since Patz1/MAZR can act as a repressor of the CD8 locus during T-cell development and might be a putative epigenetic regulator of gene expression[65], we wanted to test whether this region of homology has a role in the establishment of Patz1/MAZR-mediated protein-protein interactions. We performed a co-IP against all three differentially methylated forms of Histone H4K20 using HEK293T whole cell lysates over-expressing either Myc-BTB or Myc-MAZR. Western blot analysis showed that full length Patz1/MAZR but not the BTB domain of c-Krox can interact with mono-, di- or tri-methylated Histone H4K20 (Figure 4.9):
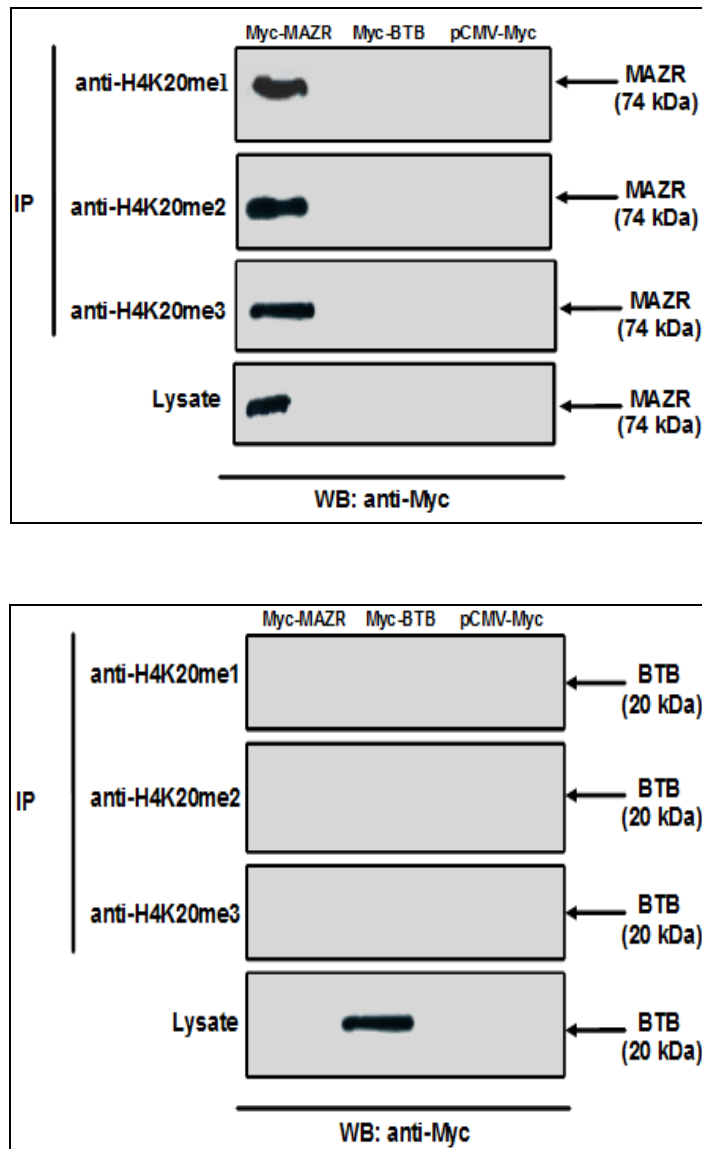
Figure 4.9: The co-IP of Myc-MAZR with differentially methylated froms of Histone H4K20 in HEK293T cells. Whole cell lysates prepared from cells over-expressing either Myc-MAZR or Myc-BTB were immunoprecipitated using antibodies against the mono-(H4K20me1), di-(H4K20me2) and tri-methylated (H4K20me3) forms of Histone H4K20. The immunocomplexes were analyzed by Western blotting using anti-Myc antibodies. Full-length MAZR successfully binds to all methylated forms of H4K20 (upper panel), whereas the BTB domain of c-Krox fails to associate with them (lower panel). 20 μg of whole cell lysate per lane (in the sub-panels captioned "Lysate") was used as input control.

This finding not only confirms the sequence-specificity of the Patz1/MAZR-p53 interaction but also suggests that such physical associations might be subjected to epigenetic regulation.

4.4 Computational Modeling of MAZR001 Reveals
the Presence of a putative Binding Pocket in the Zinc Finger Domain

In contrast to the common belief that the conserved N-terminal BTB domain is crucial for the establishment of protein-protein interactions for the BTB/ZF family[44], our findings so far have revealed no significant role for this region regarding Patz1/MAZR-p53 binding.

In the light of this information, we turned our focus on the second major domain of MAZR001 and decided to investigate, whether it's the C-terminal zinc fingers that are contributing to the physical association of Patz1/MAZR with p53. To have a better understanding of the binding mechanics, a former member of the our lab, Jitka Eryılmaz, prepared a computational homology model of the mouse MAZR001 zinc finger domain, which consists of 7 individual C_2H_2-type zinc fingers separated by short linker regions (Figure 4.10):
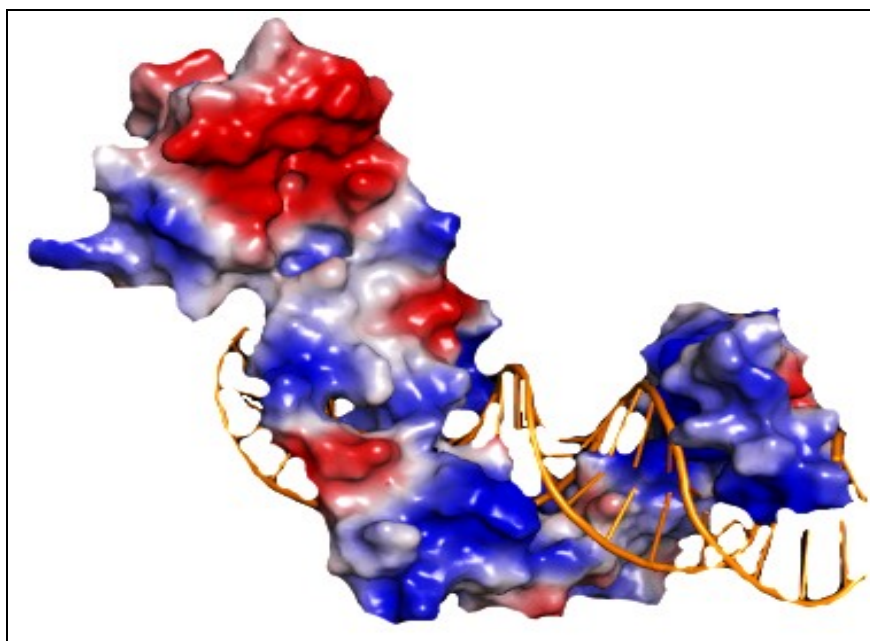

Figure 4.10: The computational homolgy model depicting the zinc finger domain of mouse MAZR001 in complex with double-stranded DNA. The positively-charged residues (shown in blue) of the individual zinc fingers bind to the negatively-charged DNA (yellow strands) via charge-mediated interactions, whereas negatively charged clusters (shown in red) tend to face away from DNA.

Upon closer inspection the model hinted at the presence of a cavity-like structure constituted by the linker region connecting the 6th and the 7th zinc fingers of MAZR001. The formation was predicted to be 9 A in diameter and has a highly negative surface-charge density (Figure 4.11):
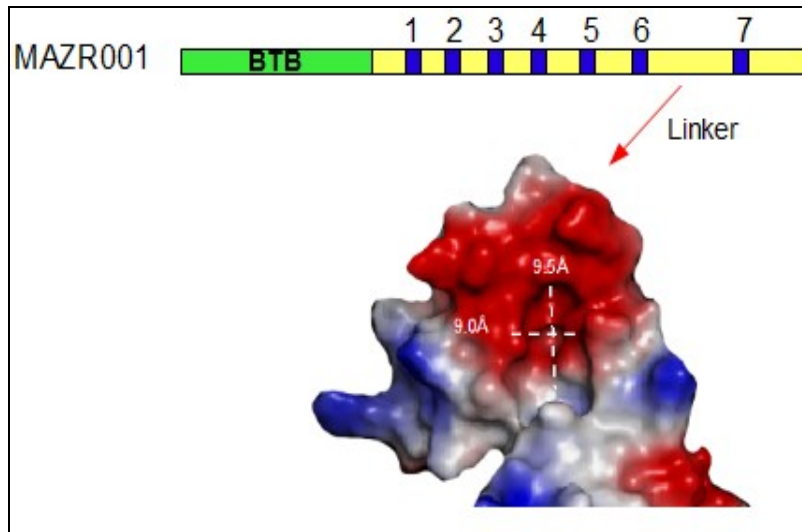
Figure 4.11: The computational homology model of the linker connecting the 6th and the 7th zinc fingers of MAZR001. The folding pattern of the region resembles that of a pocket. The diagram above the model represents the protein structure of MAZR isoform 001 (Green box: BTB domain, Blue boxes: Zinc fingers, Yellow boxes: Linker regions).

The structure of the negatively-charged cavity resembled that of a binding pocket, where a favorable environment to mediate BTB-domain-independent protein-protein interactions can be created. To test this prediction, Jitka performed virtual docking studies using the N-terminal tail of Histone H4 and the C-terminal tail of p53 as ligands for the putative binding pocket (Figure 4.12). Her predictions were in accordance with the experimental data, showing that the last lysine residue K* of the conserved "RHR/KK*" motif in both peptides can fit into the pocket and serve as a tethering site.
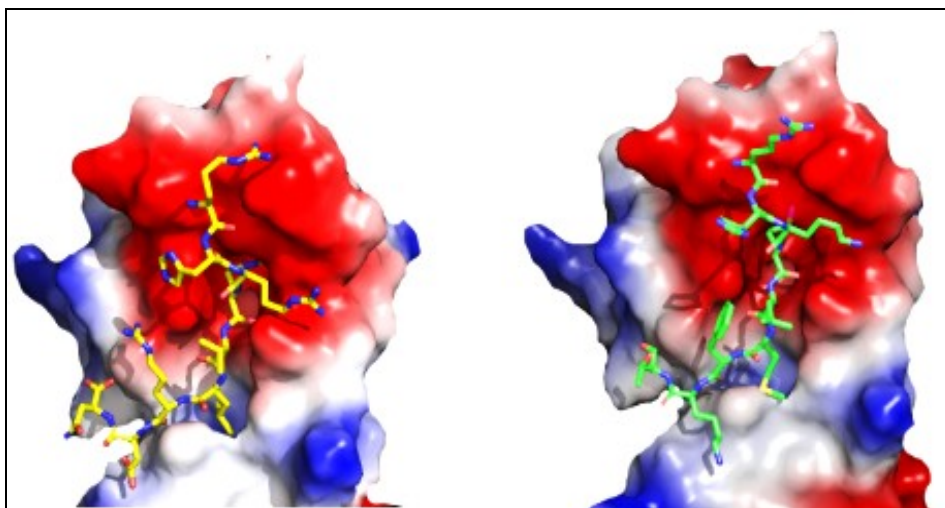
Figure 4.12: The virtual docking of Histone H4K20 and p53K382 to the putative binding pocket found within in the zinc finger domain of MAZR001. On the left, the N-terminal tail of Histone H4 (yellow molecule) containing H4K20 is fitted into the putative binding pocket depicted in red. On the left, docking is performed with the C-terminus of p53 (green molecule) containing p53K382. In both cases the lysine residues are predicted to interact favorably with the negatively-charged residues of the cavity.

4.5 Point Mutations at the Asp521 and Asp527 Residues of MAZR001 Weaken the Patz1/MAZR-p53 Interaction

The homology model of the negatively-charged linker region between the 6th and the 7th zinc fingers of MAZR001 implied that Asp521 and Asp527 in the putative binding pocket might be two of the critical residues that have important roles in the mediation of the Patz1/MAZR-p53 interaction. In order to verify these predictions, we generated the point mutant MAZRAsp521Tyr and the double mutant MAZRAsp521/527Tyr, changing the negatively-charged Asp residues into non-charged bulky Tyr residues, which should disrupt the binding (Figures 4.13 and 4.14)
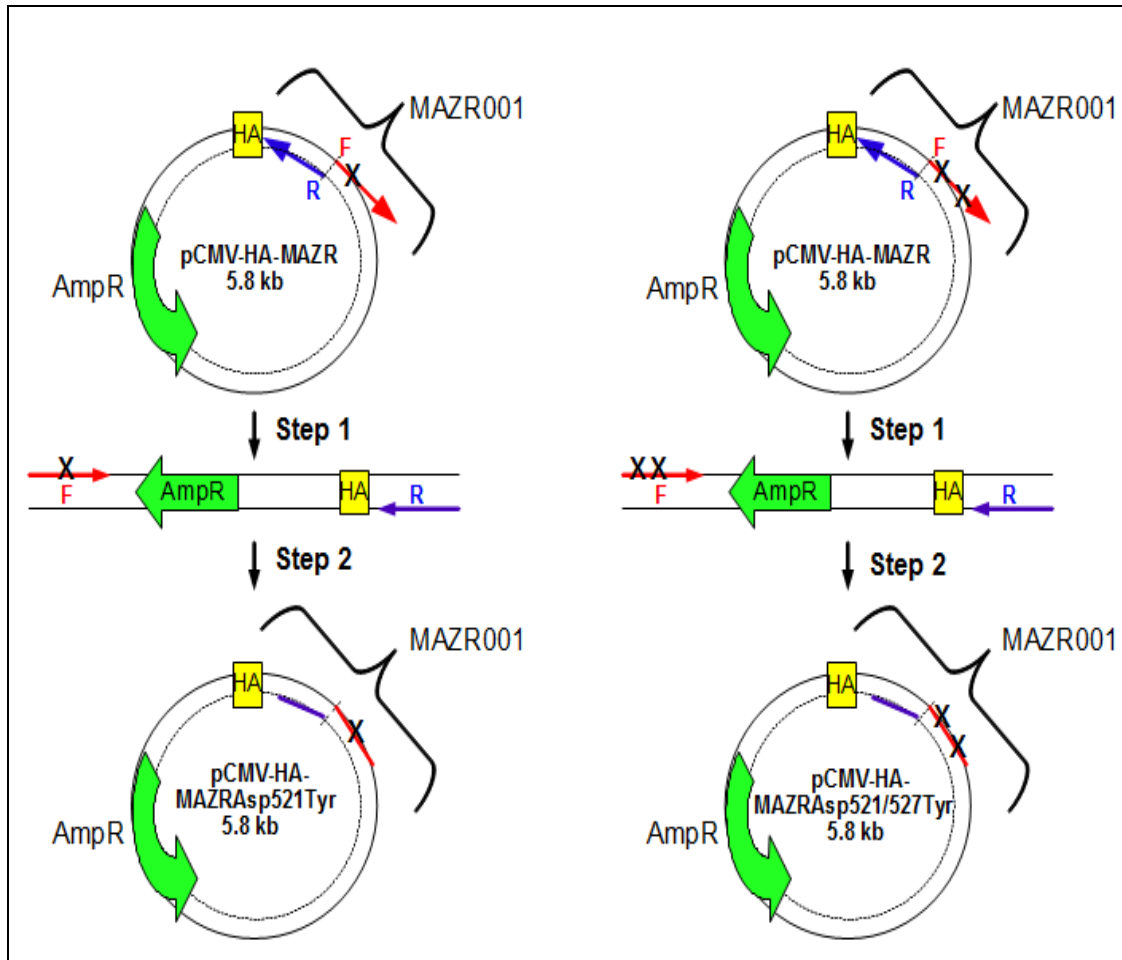
Figure 4.13: The strategy for generating the point mutant HA-MAZRAsp521Tyr (on the left) and double mutant HA-MAZRAsp521/527Tyr (on the right) by site-directed mutagenesis. In step 1, the plasmid carrying wild type MAZR001 is amplified using a mutagenic forward primer (primer denoted by the red arrow F, locations of the desired mutations are marked with an "X" on the primer) and a nonmutagenic reverse primer (denoted by the blue arrow R). In step 2, the linear PCR products harboring the mutation(s) of interest, are phosphorylated at their 5' ends by PNK and re-circularized by ligation.
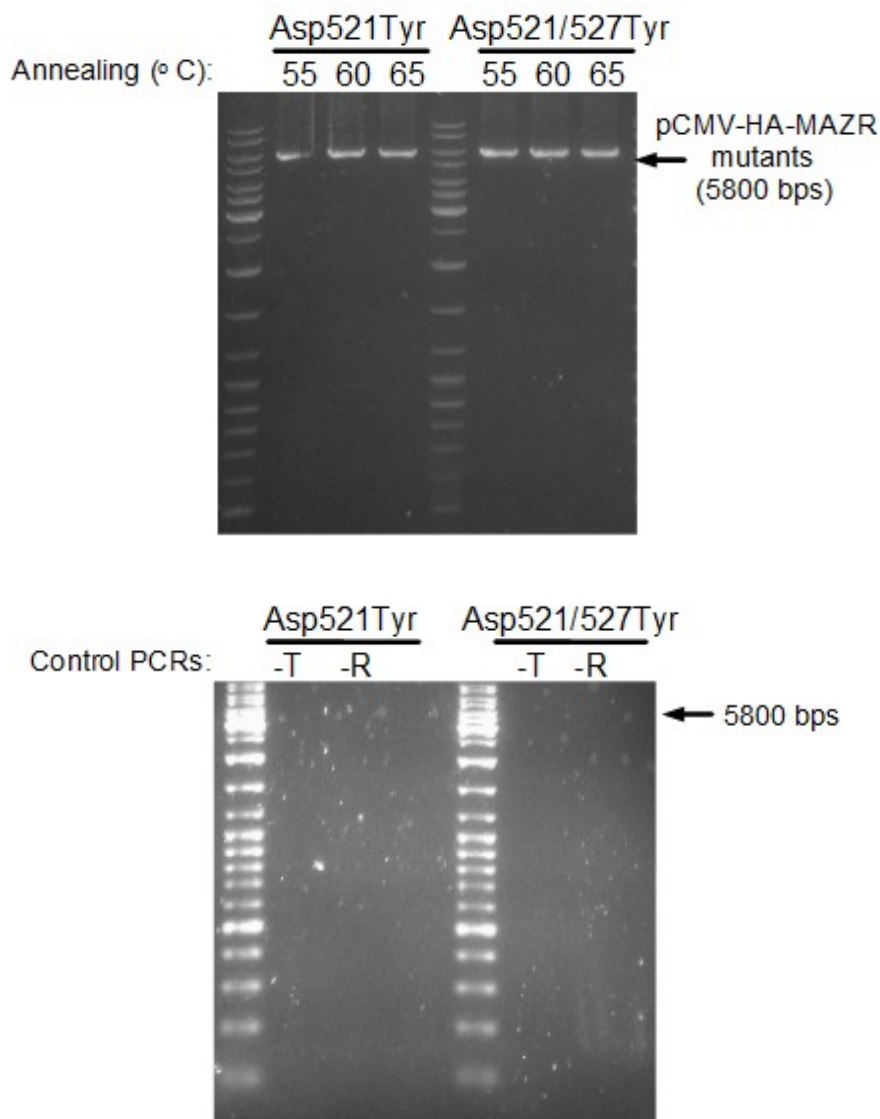
Figure 4.14: The gel photos of the mutant PCR products pCMV-HA-MAZRAsp521Tyr and pCMV-HA-MAZR521/527Tyr resulting from the amplification of pCMV-HA-MAZR (wild type) with mutagenic primers and control PCRs. Upper panel: PCR reactions described in "3.2 Methods" were carried out at annealing temperatures 55, 60 and 65 degrees C. 5 μl from each PCR mix was loaded per well to visualize the bands. Although mutant products of correct length were observed at 5.8 kb under all conditions, 60 degrees C was picked for long-term use. Bottom Panel: Control PCRs were carried out at an annealing temeperature of 60 degrees C either without the template DNA, wild type pCMV-HA-MAZR, (-T) or without the reverse primer (-R). The specificity of the reactions were confirmed since no bands were observed at 5.8 kb. The PCR products were subsequently phosphorylated at their 5' ends by PNK, re-circularized by ligation and transformed to E.coli. Plasmid DNA was isolated from single colony cultures and sent to sequencing to determine the colonies carrying the desired mutations.

In accordance with the model, a co-IP analysis in HEK293T whole cell lysates co-expressing HA-tagged Patz1/MAZR mutants and Flag-p53 revealed that the point mutation Asp521Tyr weakened the physical interaction, whereas the double mutation Asp521/527Tyr abolished the association altogether compared to the wild type (Figure 4.15):
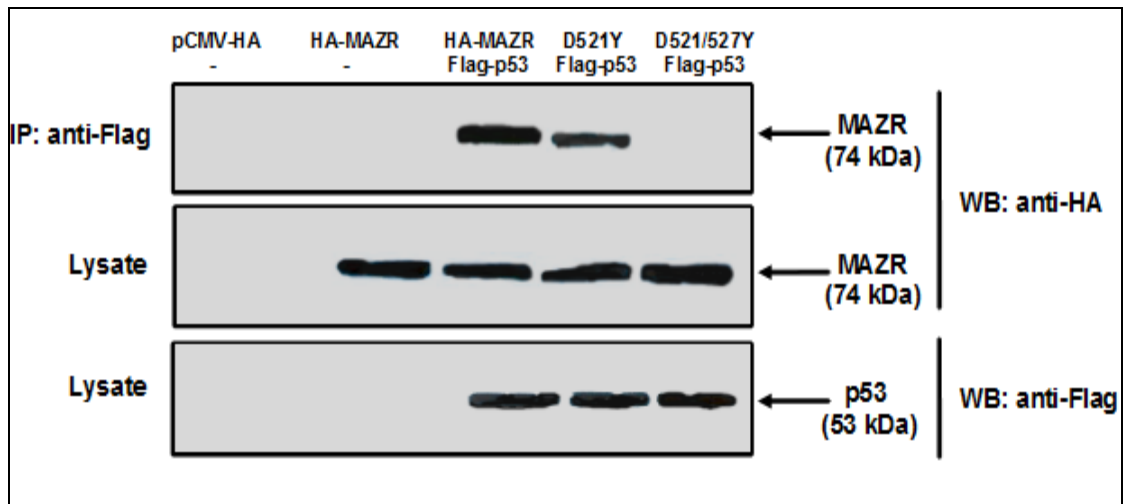
Figure 4.15: The co-IPs of ectopically-expressed wild type HA-MAZR, point mutant HA-MAZRAsp521Tyr (D521Y) and double mutant HA-MAZRAsp521/527Tyr (D521/527Y) with Flag-p53 in HEK293T cells. Whole cell lysates prepared from cells were immunoprecipitated using anti-Flag antibodies and the immunocomplexes were analyzed by Western blotting using anti-HA antibodies. 15 ug of whole cell lysate per lane (in the sub-panels captioned "Lysate") was used as input control.

4.6 Overexpression of MAZR001 Rescues HEK293T Cells from p53-induced Cell Death but Has no significant Effects on Cell Proliferation Rate

Although our findings have revealed a lot about the binding mechanics of Patz1/MAZR to p53, the physiological implications of the interaction were, yet, to be determined. Since a previous study identified Patz1/MAZR as a putative proto-oncogene in colorectal[66] and testicular cancers[67], we hypothesized that the binding may negatively regulate p53-induced apoptotic activity. To test this prediction, we transfected HEK293T cells with HA-MAZR, p53 or a combination of the two and performed trypan-blue exclusion assays at different time points following transfection to determine the live cell count over a period of 2 days. Our results showed that

MAZR001 alone has no significant effect on cell proliferation, but when co-expressed with p53, rescues cells from p53-induced cell death (Figure 4.16). The rescue, however, was incomplete, since the live cell counts remained stable over 48 hours and failed to catch up with the count of those that over-express the empty vector pCMV-HA or HA-MAZR alone starting from 16 hours post-transfection.
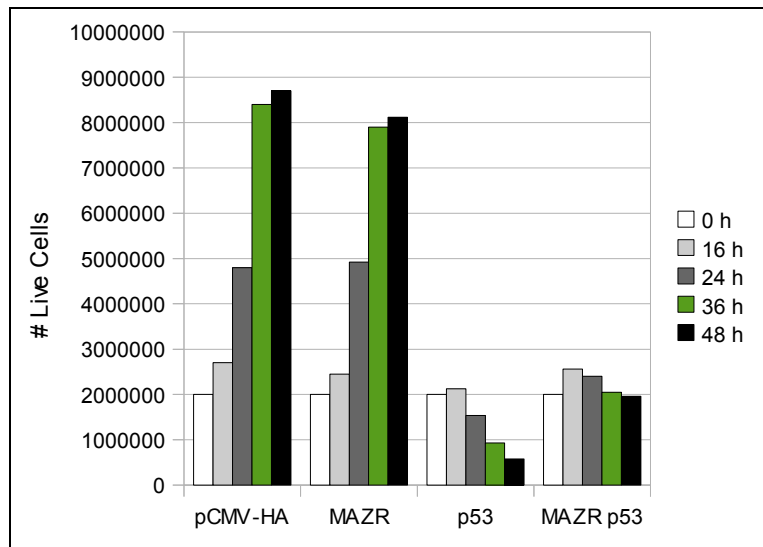
Figure 4.16: The live cell counts of HEK293T cells expressing empty vector pCMV-HA, HA-MAZR, SV40-p53 or a combination of the latter two. The number of live cells was determined 16, 24, 36 and 48 hours after transfection by trypan-blue exclusion assay.

4.7 Overexpression of MAZR001 Inhibits
DNA-damage-induced Apoptosis in DP AKR1 and VL3 Cells

To see, if the anti-apoptotic effects of the binding are cell-type-specific, we treated DP mouse lymphoma cell lines AKR1 and VL3 with 1 μM adriamycin (ADR) over a period of 12 hours to induce genotoxic stress and investigated, whether enforced expression of Patz1/MAZR can rescue the cells from p53-induced apoptosis. The dosage of the drug and the time intervals of treatment were previously determined with a time-course study by lab member Emre Deniz. The flow-cytometric analysis of 7AAD staining showed that the over-expression of MAZR decreased the sensitivity of the lymphoma cell lines to genotoxic stimuli and conferred significant protection

against apoptosis for up to 6 hours of ADR treatment (Figure 4.17). The protective effect, however, was abolished for both cell lines when the duration of treatment was prolonged to 12 hours.
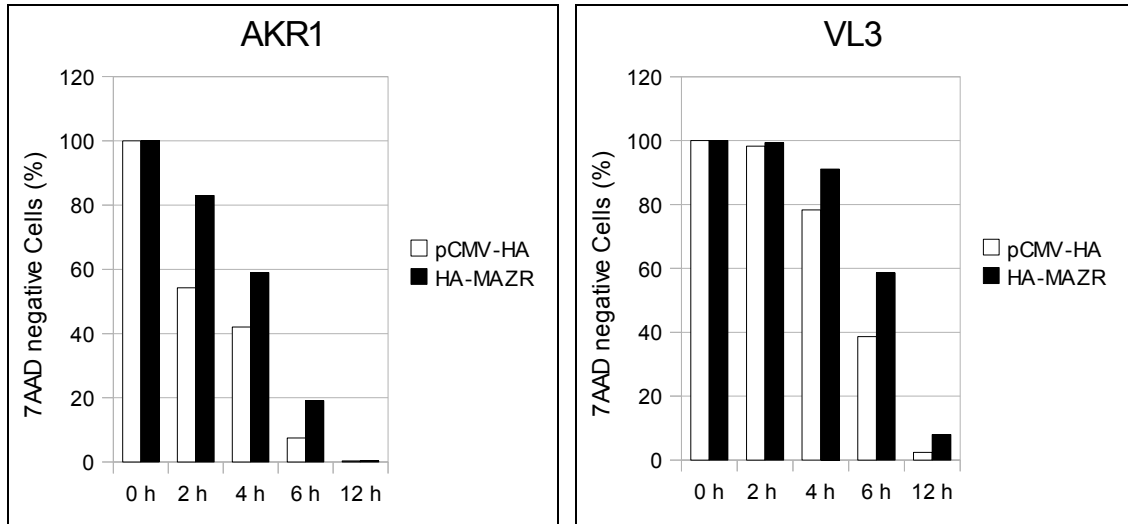
Figure 4.17: The cell survival rates analyzed by 7AAD staining in AKR1 and VL3 cells over-expressing either the empty vector pCMV-HA or HA-MAZR in response to ADR- treatment. The forced expression of MAZR confers protection against apoptosis for up to 6 hours in both cell lines.

5   DISCUSSION AND CONCLUSION

T lymphocytes constitute an important line of defense against invading pathogens and carcinogenic formations. The activation of a naive T cell in the periphery requires the engagement of the clone-specific TCR complex by a corresponding antigenic ligand. Once activated, mature T cells can proliferate rapidly and mediate the later stages of immune response, known as "adaptive immunity", by secreting regulatory cytokines or killing the afflicted host cells to prevent further propagation of the threat[7].

Since the success of adaptive immunity relies on the range of threats that can be properly identified, the immune system must generate effector cells with a diverse set of antigen-specific receptors. Such a level of diversity is maintained by combining a finite number of genomic segments to create a large repertoire of unique TCRs during maturation through a phenomenon called V(D)J somatic recombination. The process has to be tightly regulated due to the risk of generating dsDBs and disrupting genomic integrity in highly proliferative DN and DP thymocytes, which is reported to give rise to lymphomas[80, 81]. The activation of DNA damage checkpoints and the involvement of the p53-mediated DDR pathway in the regulation of somatic recombination have been previously documented[39-41].

Patz1/MAZR, also known as Zfp278, is a BTB/ZF family transcription factor that is expressed in the brain, skin and thymus. In T cells the expression is progressively down-regulated during the transition from the DN to the DP stage, and is terminated once maturation is complete[64]. The widely-studied full length isoform MAZR001 has an N-terminal BTB domain that mediates protein-protein interactions and a C-terminal zinc finger domain consisting of 7 C_2H_2-type zinc fingers. In DN thymocytes Patz1/MAZR is shown to interact with several CD8 cis-regulatory elements and induces epigenetic silencing of the locus by recruiting the nuclear co-repressor NcoR[64]. A study has revealed that the over-expression of MAZR induces variegated expression of CD8 in DP thymocytes implying a critical role in the CD4 vs. CD8 cell fate decision[65].

In addition to its involvement in the T-cell lineage commitment process, Patz1/MAZR has been identified as a culprit in colorectal[66] and testicular cancers[67], where oncogenic effects are thought to be mediated by the induction of the proto-oncogene c-Myc[68]. The down-regulation of MAZR expression by RNAi is also reported to increase the vulnerability of glioma cells to apoptotic stimuli highlighting a potential role in the regulation of cell cycle[69].

During T cell development Patz1/MAZR and the master cell cycle regulator p53 are co-expressed in DN and DP thymocytes, when dsDBs physiologically occur as a result of somatic V(D)J recombination. The pair is, again, down-regulated following the generation of a fully-assembled TCR[70]. The coordinated expression patterns with p53 and an implied effect on oncogenesis lead us to the question, whether Patz1/MAZR participates in the p53-mediated regulation of DNA damage response during somatic recombination.

Our aim in this study was to verify, whether Patz1/MAZR has a novel function in the p53-regulated steps of the DDR during T cell development. Previous studies have shown that other proto-oncogenic BTB/ZF family members, such as ZBTB2 and ZBTB5 can promote cell proliferation by binding to p53 and inhibiting its pro-apoptotic activity[73, 74]. To investigate this possibility, we performed several co-IPs in mammalian HEK293T cells and showed that over-expressed full length MAZR can interact with both ectopically-expressed- and DNA-damage-induced (by cisplatin) endogenous p53. In contrast, a conserved BTB domain obtained from another BTB/ZF member, c-Krox, failed to associate with cisplatin-induced p53, when over-expressed in HEK293T cells. The finding suggested that the BTB domain is not required for binding.

Having confirmed the occurrence of a physical association, our next goal was to determine, which domain or domains of p53 are necessary to support the interaction. The full-length protein isoform, known as p53-α, consists of 2 trans-activation domains, a proline rich domain, a DNA-binding domain, a nuclear localization signal and a basic C-terminal domain[21]. Although its function remains relatively unknown, current studies suggest that the C-terminus might be responsible from the regulation of

p53 activity[22]. To test whether the C-terminal is involved in the establishment of the interaction, we co-expressed MAZR and the truncated p53 isoform p53-β, which lacks the basic C-terminus of full length p53 in HEK293T cells. Co-IP results showed that only full length p53, but not p53-β, is able to bind to MAZR. This suggested that the presence of the basic C-terminus is required to enable binding.

The C-terminal domain of p53 and and the N-terminal tail of Histone H4 reportedly share a conserved "RHR/HK*" motif that is methylated at K* in response to DNA damage[78]. The target lysine K* is K20 in Histone H4 and K382 in p53. The K20 residue of Histone H4 can be subjected to progressive methylation, where mono- and tri-methylation are hallmarks of epigenetic silencing. Di-methylation, on the other hand, signals the mounting of DDR and inhibits transcription from the targeted loci[77]. In contrast, only the mono-methylated form from of p53K382 is reported, which is thought to result in the suppression of p53-mediated apoptotic activity[78].

Since Patz1/MAZR can act as an epigenetic repressor of the CD8 locus in DN thymocytes[65], we wanted to test, whether this region of homology can interact with MAZR. Co-IP against all three differentially methylated forms of Histone H4K20 in HEK293T cells showed that only ectopically- expressed full length MAZR, but not the BTB domain, can bind to the modified residues. Our results not only confirmed the sequence-specificity of the Patz1/MAZR-p53 interaction, but also implied that the binding might be epigenetically regulated by methylation. Furthermore, we identified an epigenetic regulation mechanism underlying the transcriptional repressor activity of MAZR. It is highly probable that Patz1/MAZR is recruited to transcriptionally inactive heterochromatin by interacting with the methylated forms of Histone H4. The question, whether it is directly involved in the methylation process, however, is yet to be answered.

Although it is assumed that the conserved N-terminal BTB domain is crucial for the establishment of protein-protein interactions for the BTB/ZF family[44], our findings have revealed no significant role for this region regarding Patz1/MAZR-p53 binding. In light of this information, we turned our attention on the zinc finger domain of MAZR001 and decided to investigate whether the C-terminal zinc fingers are

responsible from the establishment of the physical interaction between Patz1/MAZR and p53. Using computer-simulated homology modeling, we predicted the presence of an isoform 001-specific putative binding pocket generated by the linker region that connects the 6th and the 7th C2H2 zinc finger motifs in the protein. In accordance with our experimental data, virtual docking studies using the N-terminal tail of Histone H4 and the C-terminal tail of p53 as ligands showed that Histone H4K*20 and p53K*382 of the conserved "RHR/KK*" motif in both peptides can fit into the pocket and serve as a tethering site. Methylation of the lysine residues was predicted to increase the affinity of binding.

Taking the homology model as a reference point, we identified Asp495, Asp521, Asp527 and Gly538 in the putative binding pocket as critical amino acids required for the proper establishment of the Patz1/MAZR-p53 interaction. To test whether the binding pocket within the zinc finger domain is responsible from the mediation of Patz1/MAZR-p53 binding, we mutated these residues to bulky Tyr residues (confirmed by DNA sequencing) to destroy the accumulation of negative surface charges and potentially disrupt the folding pattern. Co-IPs performed with the point mutant MAZRAsp521Tyr and double mutant MAZRAsp521/527Tyr in HEK293T cells revealed that the interaction between ectopically-expressed p53 and MAZRAsp521 is weaker in comparison to that of the wild type MAZR. The double mutant MAZRAsp521/527Tyr, on the other hand, totally fails to bind to p53. Our experiments confirm the specificity of the computational model and show that several amino acids in the binding pocket in the zinc finger domain of MAZR001 is required for Patz1/MAZR-p53 binding.

In addition to deciphering the binding mechanics, we also investigated the physiological significance of the interaction. Since previous studies identified Patz1/MAZR as a putative proto-oncogene[66, 67], we hypothesized that the binding may negatively regulate p53-induced apoptotic activity. To test this prediction, we co-expressed Patz1/MAZR with p53 in HEK293T cells and performed trypan-blue exclusion assays at different time intervals to determine the live cell counts. Our results showed that Patz1/MAZR, alone, has no significant effect on cell proliferation, but when co-expressed with p53, rescues cells from p53-induced cell death. Interestingly,

however, the live cell counts remained stable over 48 hours and failed to catch up with the count of those that express the empty vector or Patz1/MAZR alone starting from 16 hours post-transfection. This effect could have been achieved by the induction of cellular senescence, hinting at a role of Patz1/MAZR in the regulation of cell cycle in HEK293T cells.

To see, if the senescence-inducing effects of the binding are cell-type-specific, we triggered p53-mediated DDR in DP mouse lymphoma cell lines AKR1 and VL3 using the genotoxic drug adriamycine and investigated, whether enforced expression of Patz1/MAZR can rescue the cells from apoptosis. We chose to use these cell lines because the DP stage of T cell development is one of the phases, where V(D)J-recombination-mediated DNA damage naturally occurs. Such a setting bears physiological relevance to our current model, where endogenous Patz1/MAZR binds to p53 and inhibits its apoptotic activity, as the developing thymocyte progresses through the DNA damage checkpoint. FACS analysis of 7AAD staining showed that the over-expression of Patz1/MAZR decreased the sensitivity of the lymphoma cell lines to apoptotic stimuli and conferred significant protection against cell death for 6 hours of adriamycine treatment. Although not included within the scope of this thesis, unpublished data from luciferase reporter assays performed in HEK293, HEK293T and Hela cell lines (by Emre Deniz) show that the binding of Patz1/MAZR inhibits the transcriptional activity of p53. All these results indicate that the physical interaction between Patz1/MAZR and p53 negatively regulates the pro-apoptotic effects of p53, and explain why Patz1/MAZR might act as a proto-oncogene.

In conclusion we have demonstrated that the BTB/ZF family member Patz1/MAZR binds to the C-terminal "RHKK*" motif of p53 through an isoform 001-specific binding pocket lying between the 6th and the 7th zinc fingers. Through computational modeling and co-IPs we have identified MAZRAsp521, MAZRAsp527 and p53Lys382 as critical amino acids that support the interaction and predicted that the interaction might be epigenetically regulated by the methylation of p53Lys382. We also showed that the binding inhibits p53-induced apoptosis in HEK293T, AKR1 and VL3 cell lines. According to our current model, this interaction occurs in DN and DP thymocytes that have undergone productive V(D)J somatic recombination and allows

them to progress through DNA damage checkpoints by suppressing p53-induced apoptosis. As DNA damage persisting through aberrant V(D)J recombination is one of the underlying causes of carcinogenesis, Patz1/MAZR appears to be a promising target for the development of new strategies in cancer therapy.

6   FUTURE WORK

In this study we identified the BTB/ZF family member Patz1/MAZR as a potential co-mediator of the p53-regulated DDR induced by somatic V(D)J recombination during T cell development. The full length isoform MAZR001 was experimentally shown to interact with the C-terminal tail of p53 in a sequence-specific manner through a binding pocket located between the 6th and the 7th C-terminal zinc fingers that was identified by computational modeling.

The putative binding pocket in the zinc finger domain was found to be exclusive to the mouse isoform 001 and couldn't be identified in the homology models of the other alternatively spliced Patz1/MAZR isoforms such as 003 or 012, which lack the signature linker region. To test the validity of the model, isoform MAZR003 was constructed by fusion PCR, but hasn't been tested in tissue culture, yet. The co-IP of the truncated isoform with p53 in HEK293T cells will reveal, whether the binding pocket, as a whole, is necessary to establish the physical interaction and supply further proof that the computational model is reliable. It would also be interesting to see, whether similar pocket-like formations exist in the zinc finger domains of Patz1/MAZR-homologs from other species or in other BTB/ZF family members. The presence of a structure responsible for protein-protein interactions in a zinc finger domain, which is classically associated with DNA binding is an unexpected, but an exciting finding. We think computational models might serve as efficient preliminary assessment tools for such purposes.

The computer-simulated model predicted the presence of several residues such as Asp495, Asp521, Asp527 and Gly538 that might be critical for the proper folding of the putative binding pocket. Although point mutants MAZRAsp495Tyr and MAZRGly538Tyr with hypothetically "dysfunctional" binding pockets were constructed, they haven't been tested in tissue culture, yet. The co-IPs of these point mutants with p53 can be carried out in HEK293T cells to further test the validity of the homology model.

Another prediction of the computational model was that the K382 residue of

p53 acts as a tethering point and is critical for the Patz1/MAZR-p53 binding. To test this prediction, p53K382 can be mutated to a bulky residue that doesn't fit into the binding pocket of MAZR and co-IPs in mammalian cell lines can be performed. Ideally such a mutant shouldn't be able to interact with MAZR. Furthermore, the interactions with the differentially methylated forms of Histone H4K20 suggest that the "RHR/KK" motif-specific binding might be a target for epigenetic regulation. p53K382 is shown to get both methylated and acetylated, but the presence of these post-translational modifications (PTMs) is mutually exclusive. Acetylation of this residue is associated with p53 activation, whereas the effects of mono-methylation hasn't been as widely studied except for a report that implies it might be responsible for suppressing p53 activity. Using PTM-specific antibodies against p53K382, co-IPs can be performed to understand, whether any of these p53 forms preferentially bind to Patz1/MAZR.

Currently our lab has undertaken efforts to investigate the biological significance of the Patz1/MAZR-p53 interaction using the CD4 SP lymphoma cell line EL4. This suspension cell line is known to form solid tumors, when injected into wild type mice and is frequently used as a model in cancer research[82]. We plan to test the proto-oncogenic properties of Patz1/MAZR by transfecting EL4 cells with the full length isoform and transplanting them into mice to see, whether the oncogenic potential of these cells are greater in comparison to those that don't express MAZR. Tumor size, growth rate and aggressiveness can be used as criteria to assess the validity of our hypothesis that Patz1/MAZR is a putative proto-oncogene. Additionally, the correlation between Patz1/MAZR expression and the frequency of aberrant V(D)J recombination can be investigated in various types of lymphomas to gain a better understanding of the nature of the interaction. According to our predictions, the over-expression of Patz1/MAZR might help cells survive through p53-mediated DNA damage checkpoints despite the unproductive rearrangement of the TCR gene locus. Such cells are likely to retain genomic instabilities and accumulate more in time to eventually transform into lymphomas.

The mechanisms governing p53 suppression by Patz1/MAZR are, still, relatively unclear. One possibility is that Patz1/MAZR exports p53 from the nucleus to repress its transcriptional activity. In order to address this, p53 and Patz1/MAZR can be

fused to fluorescent proteins and their sub-cellular locations can be tracked by co-localization studies in mammalian cell culture. Alternatively, Patz1/MAZR might be competing with another partner of p53 or preventing the generation of a PTM that is required for p53-mediated apoptotic activity. The former issue can be addressed by in vitro competition assays performed with purified proteins and co-IPs with the candidate proteins in mammalian cell culture. For the latter possibility, the inducers of the relevant PTMs can be co-transfected to mammalian cells along with Patz1/MAZR and p53 to determine, whether the modification occurs, and, if there are any notable effects of the process on p53-induced apoptotic activity.

Lastly, evidence from current literature implies that the dominant apoptotic mechanism regulating somatic recombination is inherently linked with TCR signaling. As discussed previously, the SCID-like phenotype of RAG2-/- mice can be rescued by knocking down p53, which alleviates the blockage at the DN to DP transition phase.[39, 40] It would be interesting to investigate, whether Patz1/MAZR is a part of the TCR-dependent survival signaling pathway

7 REFERENCES

1. Chen, W. The late stage of T cell development within mouse thymus. Cell Mol Immunol 1, 3-11 (2004).
2. Kondo, M., Weissman, I. L. & Akashi, K. Identification of clonogenic common lymphoid progenitors in mouse bone marrow. Cell 91, 661-72 (1997).
3. Erman, B., Feigenbaum, L., Coligan, J. E. & Singer, A. Early TCRalpha expression generates TCRalphagamma complexes that signal the DN-to-DP transition and impair development. Nat Immunol 3, 564-9 (2002).
4. Bonnet M., Ferrier P., Spicuglia S. Molecular genetics at the T-cell receptor beta locus: insights into the regulation of V(D)J recombination. Adv Exp Med Biol 650:116-32 (2009).
5. Krangel MS. Mechanics of T-cell receptor gene rearrangement. Curr Opin Immunol 21(2):133-9 (2009).
6. Weterings E., Chen DJ. The endless tale of non-homologous end joining. Cell Res. 18(1):114-24 (2008).
7. Janeway, C. Immunobiology : the immune system in health and disease (Garland Science, New York, 2009).
8. Kishimoto, H. & Sprent, J. Negative selection in the thymus includes semimature T cells. J Exp Med 185, 263-71 (1997).
9. Bommhardt, U., Beyer, M., Hunig, T. & Reichardt, H. M. Molecular and cellular mechanisms of T cell development. Cell Mol Life Sci 61, 263-80 (2004).
10. Singer A., Adoro S., Park JH. Lineage ftae and intense debate: myths, models and mechanisms of CD4- versus CD8-lineage choice. Nat Rev Immunol 8(10):788-801 (2008)
11. Bassing CH., Swat W., Alt FW. The mechanism and regulation of chromosomal V(D)J recombination. Cell 109 Suppl:S45-55 (2002).
12. Krangel MS., Carabana J., Abbaratequi I., Schlimgen R., Hawwari A. Enforcing order within a complex locus: current perspectives on the control of V(D)J recombination at the murine T-cell receptor alpha/delta locus. Immun Rev 200:224-32 (2004).
13. Tonegawa S. Somatic generation of antibody diversity. Nature 302(5909):575-81 (1983).
14. Fugmann SD. Lee AI, Shockett PE., Villey IJ, Schatz DG. The RAG proteins and V(D)J recombination: complexes, ends and transposition. Annu Rev Immunol 18:495-527 (2000).
15. Gellert M. V(D)J recombination:RAG proteins, repair factors and regulation. Annu Rev Biochem 71:101-32 (2002).
16. Desidero S., Lin WC., Li Z. The cell cycle and V(D)J recombination. Curr Top Microbiol Immunol 217:45-59 (1996).
17. Callen E., Jankovic M., Difilippantonio S., Daniel JA., Chen HT., Celeste A. et al. ATM prevents the persistence and propagation of chromosome breaks in lymhocytes. Cell 130:63-75 (2007).
18. Callen E., Nussenzweig MC., Nussenzweig A. Breaking down cell cycle checkpoints and DNA repair during antigen receptor development. Oncogene 26(56):7759-64 (2007).
19. Dujka ME., Puebla-Osorio N., Tavana O., Sang M., Zhu C. ATM and p53

are essential in the cell-cycle containment of DNA breaks during V(D)J recombination in vivo. Oncogene 29,957-965 (2010).

20. Lee J., Desiderio S. Cyclin A/CDK2 regulates V(D)J recombination by coordinating RAG-2 accumulation and DNA repair. Immunity 11(6):771-81 (1999).

21. Wang W., Rastinejad Farzan., El-Deiry W. Restoring p53-dependent tumor suppression. Cancer Biol & Therapy 2:4:Suppl. 1, S55-S63 (2003).

22. Chiarugi V., Cinelli M., Magnelli L. Acetylation and phosphorylation of the carboxy-terminal of p53: regulative significance. Oncol Res 10:55-7 (1998).

23. Vogelstein B., Kinzler KW. Achilles' heel of cancer? Nature 412:865-6 (2001).

24. Vogelstein B., Lane D., Levine AJ. Surfing the p53 network. Nature 408:307-10 (2000).

25. El-Deiry WS. Regulation of p53 downstream genes. Semin Cancer Biol 8:345-57 (1998).

26. McDonald ER., El-Deiry WS. Checkpoint genes in cancer. Ann Med 33:113-22 (2001).

27. Smith ML., Seo YR. p53 regulation of DNA excision pathways. Mutagenesis 17:149-56 (2002).

28. El-Deiry WS. Harper WJ., O'Connor PM., velculescu VE., Canman CE. et al. WAF1/CIP1 is induced in p53-mediated G1 arrest and apoptosis. Cancer Res 54:1169-74 (1994).

29. Hanawalt PC. Subpathways of nucleotide excision repair and their regulation. Oncogene 21:8949-56 (2002).

30. Leng RP., Li Y., Ma W., Wu H., Lemmers B., Chung S. et al. Pirh2, a p53-induced ubiquitin-protein ligase, promotes p53 degradation. Cell 112:779-91 (2003).

31. Haupt Y., Maya R., Kazaz A., Oren M. Mdm2 promotes rapid degradation of p53. Nature 387:296-9 (1997).

32. Marchenko ND., Zaika A., Moll UM. Death signal-induced localization of p53 protein to mitochondria. A potential role in apoptotic signaling. J Biol Chem 275:16202-12 (2000).

33. Caspari T. How to activate p53. Curr Bio 10:R315-7 (2000).

34. Lavin MF., Watters D., Song Q. Role of protein kinase activity in apoptosis. Experientia 52:979-94 (1996).

35. Yang J., Yu Y., Duerksen-Hughes PJ. Protein kinases and their involvement in the cellular responses to genotoxic stress. Mutat Res 543:31-58 (2003).

36. Ashcroft M., Taya Y., Vousden KH. Stress signals utilize multiple pathways to stabilize p53. Mol Cell Biol 2000 20:3224-33 (2000).

37. Higashimoto Y., Saito S., Tong XH., Hong A., Sakaguchi K., Appella E. et al. Human p53 is phsphorylated on serines 6 and 9 in response to DNA damaging agents. J Biol Chem 275:23199-203 (2000).

38. Shinkai Y., Rathbun G., Lam KP., Oltz EM., Stewart V., Mendelsohn M., Charron J., Datta M., Young F., Stall AM., Alt FW. RAG-deficient mice lack mature lymphocytes owing to inability to initiate V(D)J rearrangement. Cell 68:855-867 (1992).

39. Jiang D., Lenardo MJ., Zuniga-Pflücker JC. p53 prevents maturation to the CD4(+)CD8(+) stage of thymocyte differentaiation in the absence of T cell receptor rearrangement. J Exp Med 183:1923-28 (1996).

40. Nguyen TV., Puebla-Osorio N., Pang H., Dujka ME., Zhu C. DNA damage-

induced cellular senescence is sufficient to suppress tumorigenesis: a mouse model. J Exp Med 204(6):1453-1461 (2007).

41. aPerkins EJ., Nair A., Cowley DO., Van Dyke T., Chang Y., Ramsden DA. Sensing of intermediates in V(D)J recombination by ATM. Genes Dev 16:159-164 (2002).
42. Costoya J. Functional analysis of the role of POK transcriptional reppressors. Brief Fuc Genomic Proteomic 6(1):8-18 (2007).
43. de Ruijter AJ., Van Gennip AH., Caron HN. et al. Histone deacetylases (HDACs): characterization of the classical HDAC family. Biochem J 370:737-49 (2003).
44. Perez-Torrado R., Yamada D., Defossez PA. Born to bind: the BTB protein-protein interaction domain. Bioessays 28(12):1194-202 (2006).
45. Bilic, I. & Ellmeier, W. The role of BTB domain-containing zinc finger proteins in T cell development and function. Immunol Lett 108, 1-9 (2007).
46. He, X., He, X., Dave, V. P., Zhang, Y., Hua, X., Nicolas, E., Xu, W., Roe, B. A. & Kappes, D. J. The zinc finger transcription factor Th-POK regulates CD4 versus CD8 T-cell lineage commitment. Nature 433, 826-33 (2005).
47. Egawa, T. & Littman, D. R. ThPOK acts late in specification of the helper T cell lineage and suppresses Runx-mediated commitment to the cytotoxic T cell lineage. Nat Immunol 9, 1131-9 (2008).
48. Dave, V. P., Allman, D., Keefe, R., Hardy, R. R. & Kappes, D. J. HD mice: a novel mouse mutant with a specific defect in the generation of CD4(+) T cells. Proc Natl Acad Sci U S A 95, 8187-92 (1998).
49. Sun, G., Liu, X., Mercado, P., Jenkinson, S. R., Kypriotou, M., Feigenbaum, L., Galera, P. & Bosselut, R. The zinc finger protein c-Krox directs CD4 lineage differentiation during intrathymic T cell positive selection. Nat Immunol 6, 373- 81 (2005).
50. Kang, B. Y., Miaw, S. C. & Ho, I. C. ROG negatively regulates T-cell activation but is dispensable for Th-cell differentiation. Mol Cell Biol 25, 554-62 (2005).
51. Miaw, S. C., Choi, A., Yu, E., Kishikawa, H. & Ho, I. C. ROG, repressor of GATA, regulates the expression of cytokine genes. Immunity 12, 323-33 (2000).
52. Omori, M., Yamashita, M., Inami, M., Ukai-Tadenuma, M., Kimura, M., Nigo, Y., Hosokawa, H., Hasegawa, A., Taniguchi, M. & Nakayama, T. CD8 T cellspecific downregulation of histone hyperacetylation and gene activation of the IL-4 gene locus by ROG, repressor of GATA. Immunity 19, 281-94 (2003).
53. Piazza, F., Costoya, J. A., Merghoub, T., Hobbs, R. M. & Pandolfi, P. P. Disruption of PLZP in mice leads to increased T-lymphocyte proliferation, cytokine production, and altered hematopoietic stem cell homeostasis. Mol Cell Biol 24, 10456-69 (2004).
54. Baron BW., Nucifora G., McCabe N. et al. Identification of the gene associated with the recurring chromosomal translocations t(3;14)(q27;q32) and t(3;22)(q27;q11) in B-cell lymphomas. Proc Natl Acad Sci USA 90:5262-6 (1993).
55. Dent AL., Shaffer AL., Yu X. et al. Control of inflammation, cytokine expression, and germinal center formation by BCL-6. Science 276:589-92 (1997).
56. Niu H. The proto-oncogene BCL-6 in normal and malignant B cell

development. Hematol Oncol 20:155-66 (2002).

57. Offit K., Lo Coco F., Louie DC. et al. Rearrangement of the Bcl-6 gene as a prognostic marker in diffuse large-cell lymphoma. N Engl J Med 331:74-80 (1994).

58. Dhordain P., Albagli O., Honore N. et al. Colocalization and heteromerization between the two human oncogene POZ/zinc finger proteins, LAZ3 (BCL6) and PLZF. Oncogene 19:6240-50 (2000).

59. Davies JM., Hawe N., Kabarowski J. et al. Novel BTB/POZ domain zinc-finger protein, LRF, is a potential target of the LAZ-3/BCL-6 oncogene. Oncogene 18:365-75 (2005).

60. Schubot FD., Tropea JE., Waugh DS. Structure of the POZ domain of human LRF, a master regulator of oncogenesis. Biochem Biophys Res Commun 351:1-6 (2006).

61. Maeda T., Hobbs RM., Merghoub T. et al. Role of the proto-oncogene Pokemon in cellular transformation and ARF repression. Nature 433:278-85 (2005).

62. Mastrangelo T., Modena P., Tornielli S., Bullrich F., Testi MA., Mezzelani A., Radice A., Azzarelli A., Pilotti S., Croce CM., Pierotti MA., Sozzi G. A novel zinc finger gene is fused to EWS in small round cell tumor. Oncogene 19(33):3799-3804 (2000).

63. Fedele M., Benvenuto G., Pero R., Majello B., Battista S., Lembo F., Vollono E., Day PM., Santoro M., Lania L., Bruni CB., Fusco A., Chiariotti L. A novel member of the BTB/POZ family, PATZ, associates with the RNF4 RING finger protein and acts as a transcriptional repressor. J Biol Chem 275(11):7894-901 (2000).

64. Sakaguchi S, Hombauer M, Bilic I, Naoe Y, Schebesta A, Taniuchi I, Ellmeier W. The zinc-finger protein MAZR is part of the transcription factor network that controls the CD4 versus CD8 lineage fate of double-positive thymocytes. Nat Immunol. 11(5):442-8 (2010).

65. Bilic, I., Koesters, C., Unger, B., Sekimata, M., Hertweck, A., Maschek, R., Wilson, C. B. & Ellmeier, W. Negative regulation of CD8 expression via Cd8 enhancer-mediated recruitment of the zinc finger protein MAZR. Nat Immunol 7, 392-400 (2006).

66. Tian X, Sun D, Zhang Y, Zhao S, Xiong H, Fang J. Zinc finger protein 278, a potential oncogene in human colorectal cancer. Acta Biochim Biophys Sin (Shanghai) 40(4):289-96 (2008).

67. Fedele M., Franco R., Salvatore G., Paronetto MP., Barbagallo F., Pero R., Chiariotti L., Sette C., Tramontano D., Chieffi G., Fusco A., Chieffi P. PATZ1 gene has a critical role in the spermatogenesis and testicular tumours. J Pathol 215(1):39-47 (2008).

68. Kobayashi A, Yamagiwa H, Hoshino H, Muto A, Sato K, Morita M, Hayashi N, Yamamoto M, Igarashi K. A combinatorial code for gene expression generated by transcription factor Bach2 and MAZR (MAZ-related factor) through the BTB/POZ domain. Mol Cell Biol 20(5):1733-46 (2000).

69. Tritz R., Mueller BM., Hickey MJ., Lin AH., Gomez GG., Hadwiger P., Sah DW., Muldoon L., Neuwelt EA., Kruse CA. siRNA Down-regulation of the PATZ1 Gene in Human Glioma Cells Increases Their Sensitivity to Apoptotic Stimuli. Cancer Ther 6(B):865-876 (2008).

70. www.immgen.org

71. Sambrook, J. & Russell, D. W. Molecular cloning : a laboratory manual (Cold Spring Harbor Laboratory Press, Cold Spring Harbor, N.Y., 2001).
72. Choi, W.I., Jeon, B.N., Yun, C.O., Kim, P.H., Kim, S.E., Choi, K.Y., Kim, S.H., and Hur, M.W. Proto-oncogene FBI-1 represses transcription of p21CIP1 by inhibition of transcription activation by p53 and Sp1. J Biol Chem 284, 126 (2009).
73. Jeon, B.N., Choi, W.I., Yu, M.Y., Yoon, A.R., Kim, M.H., Yun, C.O., and Hur, M.W. ZBTB2, a novel master regulator of the p53 pathway. J Biol Chem 284, 17935-946 (2009).
74. Koh DI., Choi WI., Jeon BN., Lee CE, Yun CO., Hur MW. A novel POK family transcription factor, ZBTB5, represses transcription of p21CIP1 gene. J Biol Chem 284(30):19856-66 (2009).
75. Bourdon JC. p53 and its isoforms in cancer. BR J Cancer 97(3):277-82 (2007).
76. Shi et al. Modulation of p53 Function by SET8-mediated Mathylation at Lysine 382. Mol. Cell. 27(4):636-649 (2007).
77. Upadhyay AK, Cheng X. Dynamics of histone lysine methylation: structures of methyl writers and erasers. Prog Drug Res. 67:107-24 (2011).
78. Shi X, Kachirskaia I, Yamaguchi H, West LE, Wen H, Wang EW, Dutta S, Appella E, Gozani O. Modulation of p53 function by SET8-mediated methylation at lysine 382. Mol Cell 27(4):636-46 (2007).
79. Kachirskaia I, Shi X, Yamaguchi H, Tanoue K, Wen H, Wang EW, Appella E, Gozani O. Role for 53BP1 Tudor domain recognition of p53 dimethylated at lysine 382 in DNA damage signaling. J Biol Chem. 283(50):34660-6 (2008).
80. Kang YH, Son CY, Lee CH, Ryu CJ. Aberrant V(D)J cleavages in T cell receptor beta enhancer- and p53-deficient lymphoma cells. Oncol Rep. 23(5):1463-8 (2010).
81. Dadi S, Le Noir S, Asnafi V, Beldjord K, Macintyre EA. Normal and pathological V(D)J recombination: contribution to the understanding of human lymphoid malignancies. Adv Exp Med Biol. 650:180-94 (2009).
82. Masunaga S, Nagasawa H, Liu Y, Sakurai Y, Tanaka H, Kashino G, Suzuki M, Kinashi Y, Ono K. Evaluation of the radiosensitivity of the oxygenated tumor cell fractions in quiescent cell populations within solid tumors. Radiat Res. 174(4):459-66 (2010).
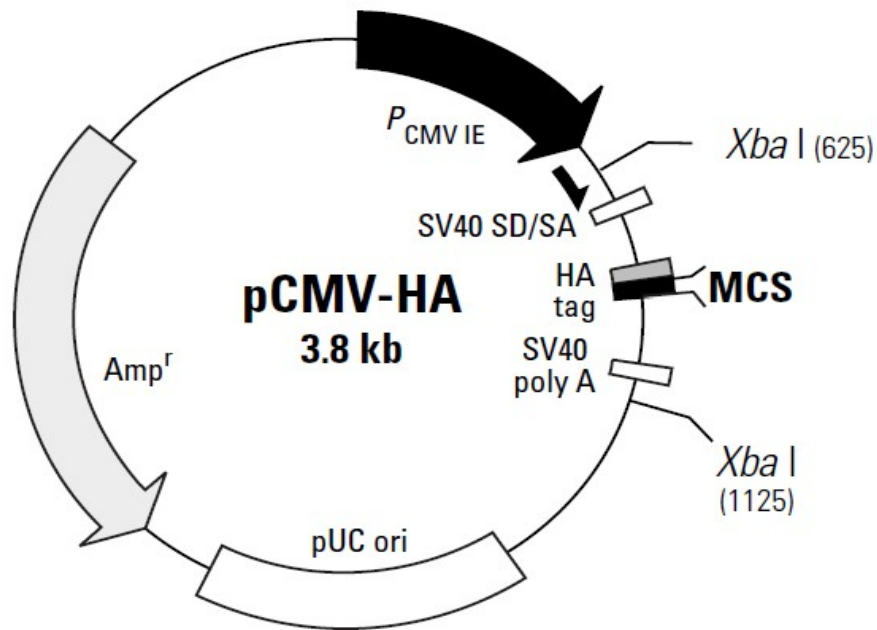
APPENDIX A- VECTOR MAP
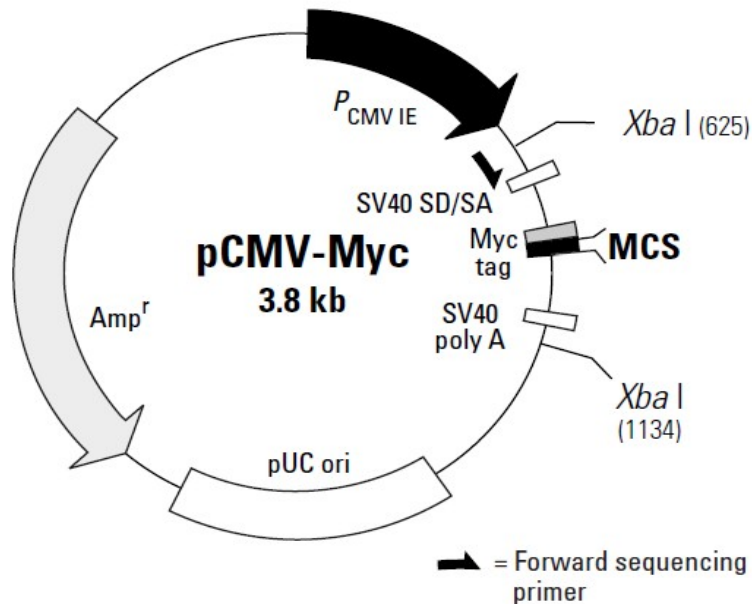
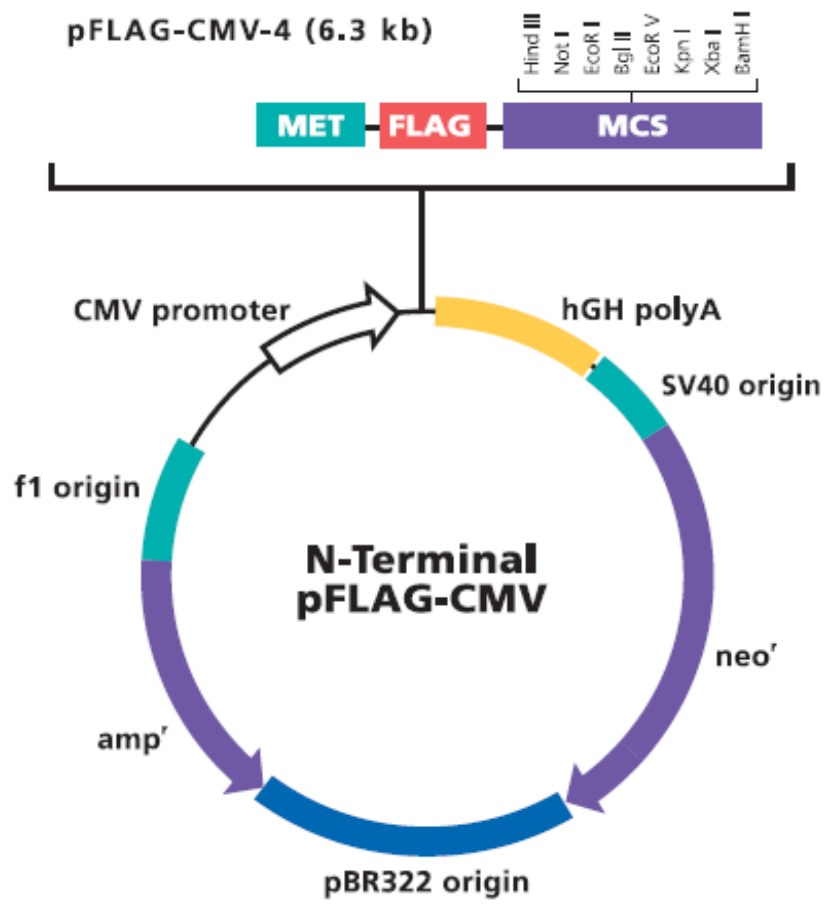**Location of features:**
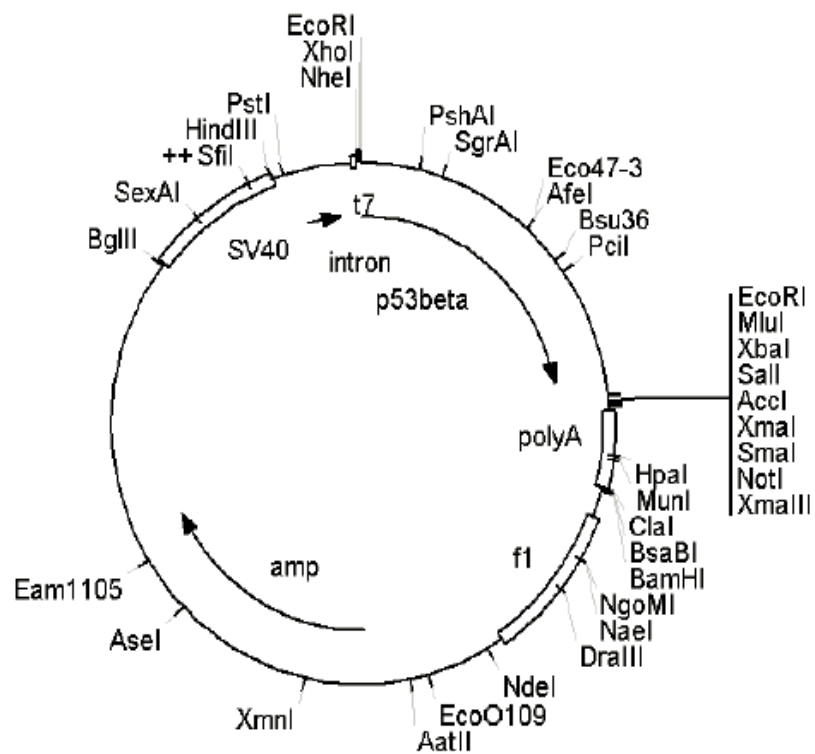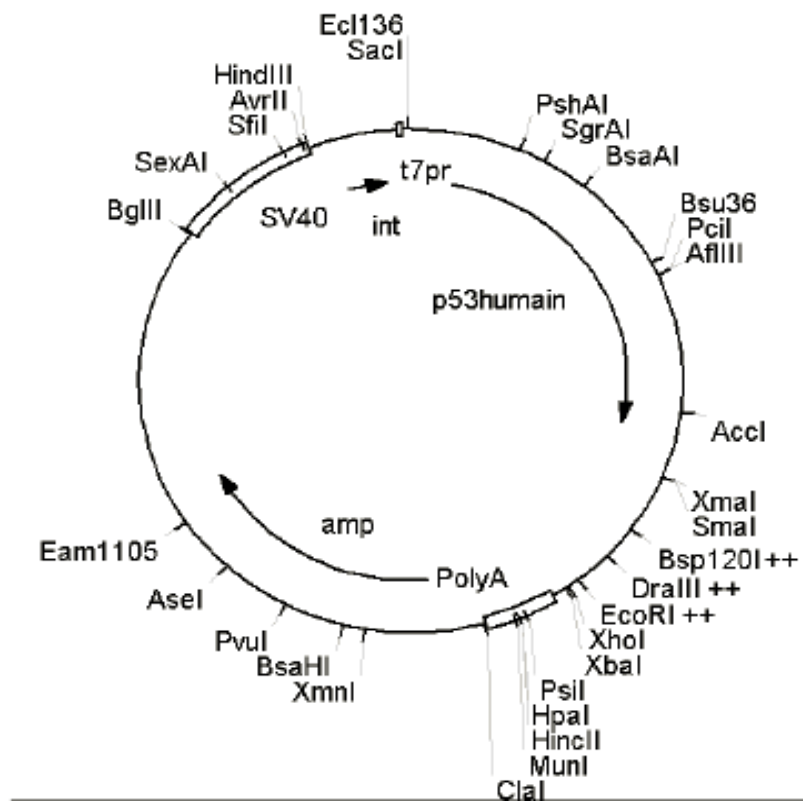- Immediate early cytomegalovirus promoter ($P_{CMV\ IE}$):
    Enhancer region: 27–431
    TATA Box: 520–526
    Transcription start point: 549
- Intron (SV40 splice donor/splice acceptor):
    SV40 late 19s mRNA intron: 672–702
    Modified SV40 late 16s mRNA intron: 672–768
- Myc epitope tag with start codon (ATG): 829–867
- Multiple Cloning Site: 881–921
- SV40 polyadenylation signal:
    Polyadenylation signal: 1053–1058
    mRNA 3' end: 1072
- pUC plasmid replication region: 1545–2188
- Ampicillin resistance (β-lactamase) gene:
    Promoter:
        -35 region: 3266–3261
        -10 region: 3243–3238
    Transcription start point: 3231
    Ribosome binding site: 3208–3204
    β-lactamase coding sequences:
        Start codon (ATG): 3196–3194
        Stop codon (TAA): 2338–2336
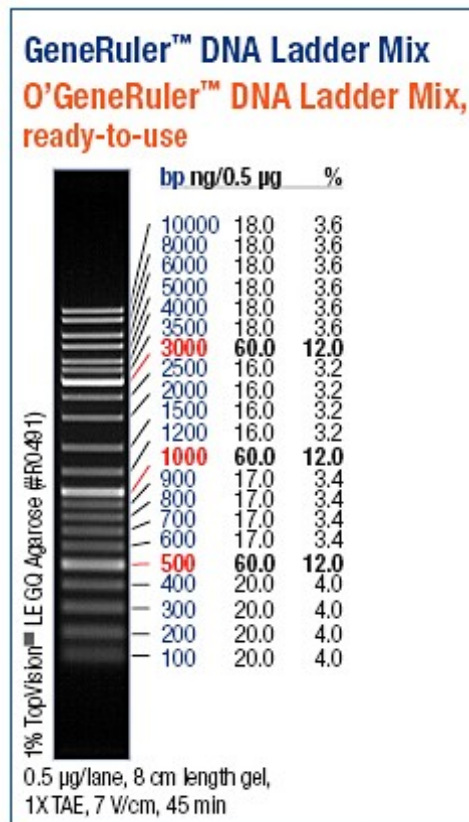
Location of features:
- Immediate early cytomegalovirus promoter ($P_{CMV\ IE}$):
  - Enhancer region: 27–431
  - TATA Box: 520–526
  - Transcription start point: 549
- Intron (SV40 splice donor/splice acceptor):
  - SV40 late 19s mRNA intron: 672–702
  - Modified SV40 late 16s mRNA intron: 672–768
- HA epitope tag with start codon (ATG): 829–858
- Multiple Cloning Site: 872–912
- SV40 polyadenylation signal:
  - Polyadenylation signal: 1044–1049
  - mRNA 3' end:1063
- pUC plasmid replication region: 1536–2179
- Ampicillin resistance (β-lactamase) gene:
  - Promoter:
    - -35 region: 3257–3252
    - -10 region: 3234–3229
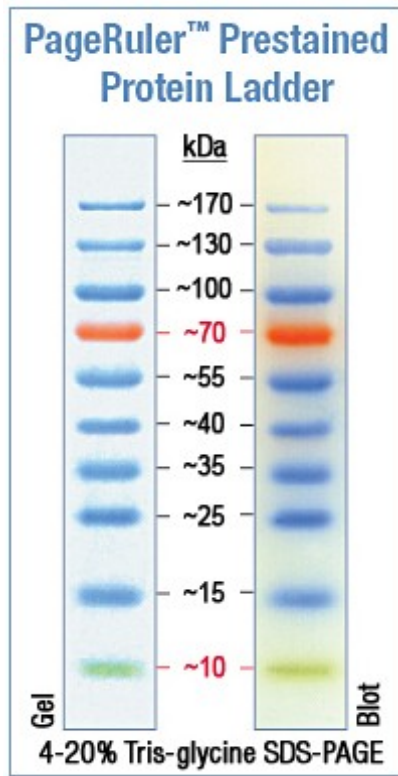 - Transcription start point: 3222
  - Ribosome binding site: 3199–3195

pFLAG-CMV-4 (6.3 kb)

HindIII Not I EcoR I Bgl II EcoR V Kpn I Xba I BamH I

MET — FLAG — MCS

CMV promoter

hGH polyA

SV40 origin

f1 origin

N-Terminal
pFLAG-CMV

neo'

amp'

pBR322 origin

DNA Molecular Weight Marker

GeneRuler DNA Ladder Mix
Fermentas, Germany

Protein Molecular Weight Marker

PageRuler Prestained Protein Ladder
Fermentas, Germany